C'e' una verità elementare, la cui ignoranza

uccide innumerevoli idee e splendidi piani:

nel momento in cui uno si impegna a fondo, anche la

provvidenza allora si muove. Infinite cose accadono per

aiutarlo, cose che altrimenti mai sarebbero

avvenute...Qualunque cosa tu possa fare,
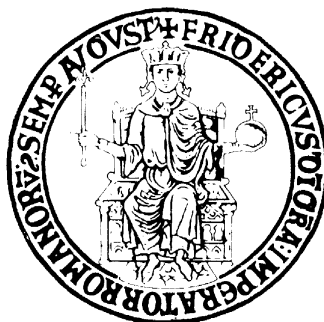
o sognare di poter fare,

INCOMINCIALA.

L'audacia ha in se' genio, potere e magia.

Incomincia adesso.

(W. Goethe)

UNIVERSITA' DEGLI STUDI DI NAPOLI *"FEDERICO II"*

FACOLTA' DI FARMACIA

Dr. Salvatore Di Maro

XXI Ciclo di Dottorato in Scienza del Farmaco

Efficient Solid-Phase Synthesis of FK228 Analogues as Potent Antitumoral Agents

Tutor:

Ch. mo Prof.
Paolo Grieco

Coordinatore:

Ch. ma Prof.ssa
Maria Valeria D'Auria

1. THE FEATURES OF CANCER

The last quarter century of cancer research has indicated the tumorigenesis as a multi-steps process involving dynamic changes in the genome and its regulation.[1] Despite the large number of cancer types actually described, most of them share in common the manifestation of six essential alterations: self sufficiency in growth signals, insensitivity to growth-inhibitory signals, evasion of programmed cell death (apoptosis), limitless replicative potential, sustained angiogenesis and tissue invasion and metastasis. Each of these physiological changes is considered as a novel capabilities acquired during tumor development that preserve the neoplastic cell from the anticancer defense mechanisms.[2]
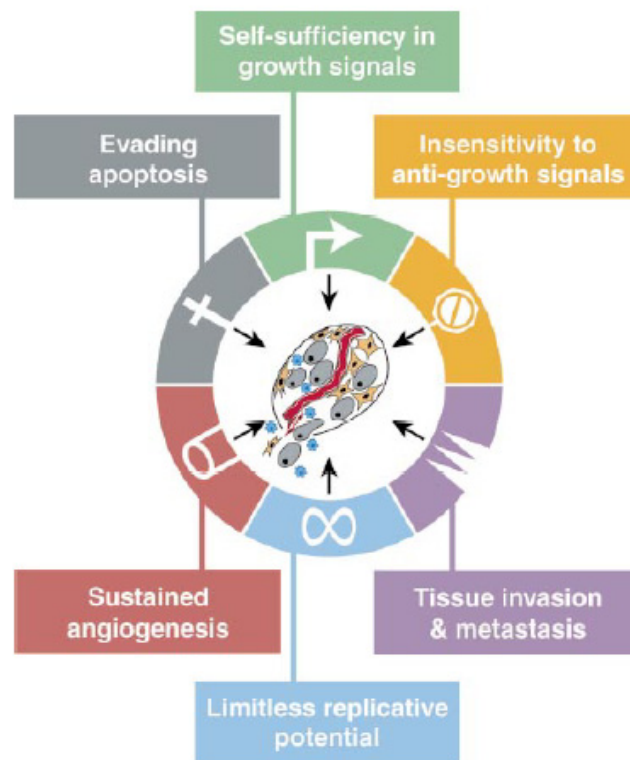

Figure 1. The six acquired capabilities of cancer cells

1.1 Self sufficiency in growth signals.

The autonomy of the proliferation of tumor cells from the growth signals was the first of the six acquired capabilities to be disclosed by cancer researchers. It has been widely demonstrated that normal cells can move from the quiescent state into a proliferative active state under the regulation of the growth signals. The normal proliferative process can be simplified in three main steps:

1.   Growth extracellular signals that bring the message (diffusible growth factor, extracellular matrix component and cell-to-cell adhesion/interaction molecules)

2.   Transmembrane receptors that transmit the signal into the cells

3.   Intracellular circuits that translate the messages into action

To achieve growth-signals autonomy, three common strategies have been highlighted involving modification of at least one of the mechanisms above described. While the proliferation of normal cells is regulated from the presence of growth extracellular signals released from another cell type (heterotypic signal), tumor cells develop the ability to produce growth-factors to which they are responsive bypassing the dependence on growth-factors released from other cells within the tissue.[3]

Also, the transmembrane receptors can be themselves targets of deregulation during tumorigenesis, being overexpressed or structural altered. The result is that cancer cells become hyperresponsive to levels of growth factors that normally would not stimulate proliferation.[3] Tumor cells can also modify the cell surface receptor system promoting the types of extracellular matrix receptors (integrins) that transmit pro-growth signals.[4] Integrins connect the cells with the extracellular matrix (ECM) and when

activated by binding specific moiety of the ECM they can stimulate the cells to move from the quiescent state to the active proliferative state conferring them resistance to apoptosis. When integrins do not recognize these extracellular links the cells undergo cycle arrest and apoptosis.[4]

The third mechanism to acquire growth factors autonomy derives from alterations of the intracellular circuits that receive and process the growth signals emitted from the transmembrane receptors. The SOS-Ras-Raf-MAPK cascade revealed to play a critical role in this strategy, in fact in about 25% of tumors the Ras proteins are present in altered form that enable them to start the stream of events for the proliferative activation without any dependence from their normal upstream signals. In some other case the presence of modifications on other components of the growth pathway signals of Ras[5] or on the cross-talking connections with Ras can be hypothesized as alternative mechanism to alter the intracellular circuits.[6]

An emerging theory to further explain the acquisition of the growth signals autonomy of the cancer cells is the cell-to-cell growth control (heterotypic regulation), which appears to operate in the majority of human tumors as well as they do for normal cells.[7]

1.2 Insensitivity to growth-inhibitory signals.

In normal tissues the normal cellular quiescent state and tissue homeostasis is maintained by the activity of antiproliferative signals that interact with transmembrane receptors coupled to intracellular circuits. Apart from the nature of the growth inhibitory signals (soluble growth factors, immobilized in the extracellular matrix or on the surface of the nearby cells), they induce cellular growth arrest though two main mechanisms.

7

First, the antiproliferative signals can force the cells to move from the active state to the quiescent state (G_o) where they can move back when the extracellular signals permit. In alternative strategy the cells can be forced into postmitotic state where them acquire specific differentiation-associated trails. Evading these anti-proliferative signals let the cancer cells to proliferate. The components governing the transit of the cell from the G_1 to S phase (TGFβ/pRb/E2Fs/CDK4/ p15^{INK4B}/p21) are mainly responsible for the sensibility of the cell to the anti-growth signals.[8] It follows that the disruption of this circuits altering the expression or the functionality of the single components can be considered as one of the strategy for the cells to become not responsive to growth-inhibitory signals.[9]

Our tissues can also regulate cell multiplication by instructing cells to enter irreversibly into postmitotic, differentiated state. Recently, several mechanisms of the tumor cells to avoid terminal differentiation have been reported.[10] However, the components involved in this process are not yet completely understood and required further investigation.

1.3 Evasion of programmed cell death (apoptosis).

The normal tissue homeostasis is also regulated by the programmed cell death (Apoptosis), which is normally present in latent form in all cell types through the body.

When activated by a variety of physiologic signals, the apoptotic program can start a series of events that result in the cell death by disrupting the cell membranes, breaking down the cytoplasmatic and nuclear skeleton, degrading the chromosomes and fragmenting the nucleus. The apoptotic circuit can be divided into two main classes of components, sensors and effectors. The extracellular factors (IGF-1/IGF-

2/FAS/TNFα), their receptors (IGF-1R/FAS/TNF-R1)[11] and intracellular sensors[12] monitor the cell conditions activating the effectors which produce the apoptotic death. An important effector of the apoptotic program is the p53 (also known as DNA-guardian) that can respond to DNA damages upregulating expression of proapoptotic factors such as Bax, that stimulates mitochondria to release cytochrome C, a potent catalyst of apoptosis.

Other well documented effectors of the apoptosis are the intracellular proteases termed caspases, that activated from sensors like FAS or effectors like p53 and cytochrome C can selectively destruct subcellular structures and genome. [13]

The mutation of the p53 suppressor gene and its resulting loss of a capability to monitor the DNA state has been observed in greater than 50% of human cancer forms and is considered as one of the key component to understand the strategies adopted by the cancer cells to acquire resistance to apoptosis.[14]

1.4 Limitless replicative potential.

The three acquired capabilities above described lead to an uncoupling of a cells growth program from the state of its environment. However, the understanding of these mechanisms have still left unsolved questions about the expansive tumor growth. Studies performed on cell cultures have widely demonstrated that all types of normal mammalian cells carry an intrinsic and independent cell-autonomous program that limits their proliferation.[15]

The senescence of cultured human fibroblasts can be overcome by disabling the pRb and p53 suppressor proteins, enabling these cells to continue proliferating until they enter into state named crisis. This phase is characterized by massive cell death and the occasional emergence of modified cell (1 in 10^7) that has acquired the ability to multiply

without limits (immortalization). The crisis state has been described as the consequence of a mechanism termed "counting device" , which is indicated as the progressive loss of base pairs in the terminal region of the chromosomes (also known as telomeres) during the replicative generations. The shortening of the telomeres disable them to protect the ends of the chromosomal DNA, which can participate in the end-end chromosomal fusion, producing the karyotipic disarray associated with the death of the affected cells.[16]

Alternatively, most of the human tumor cells appear to maintain intact the telomeres[17] probably by upregulating the expression of enzymes that protect the telomeres by adding hexanucleotide units at the end of DNA. This acquired phenotypic capability is clearly a key component to explain the unlimited replication of tumor cells, however further investigations need to be performed on the phenomenon of senescence and its circumvention which could potentially provide more information about the "Limitless replicative potential".[18]

1.5 Sustained angiogenesis.

The normal cells reside within 100 μM of capillary blood vessels in order to receive the nutrient and the oxygen necessary to guarantee their survival and functions. In the course of organogenesis this correct distance is carefully regulated by a complex set of events termed angiogenesis. The balance between the positive and negative signals encourage or block angiogenesis. Soluble inducer (VEGF/FGF1/2) and inhibitor (thrombospondin-1) factors along with their tyrosine kinase receptors displayed on the surface of the endothelial cells[3,19] represent one class of these signals. Also integrins and adhesion molecules mediating cell-matrix contribute maintaining this balance.[20]

The ability of the tumor cells to induce and sustain the angiogenesis is not evident in the preliminary phase of the tumorigenesis[21], but it seems to be acquired in successive steps of the tumor development. The angiogenic switch from vascular quiescence can be achieved by different strategies. One of them involves altered gene transcription of the positive control and negative signals. Alternatively in some cell types the downregulation of the endogenous inhibitor signal thrombospondin-1 has been associated with the loss of p53 function, which occurs in most of the human tumors.[22] Moreover, activation of *ras* oncogene has been correlated with the upregulation of VEGF expression in certain types of cells.[23] Despite that the knowledge of this process is still very limited, it is already clear that tumor angiogenesis offers an attractive target therapeutic for the treatments of many tumors.

1.6 Tissue invasion and metastasis.

Primary human tumors acquire the ability to generate pioneer cells that move out invading adjacent tissue or distant sites. This process of colonization of new terrain in the body termed metastasis let the cancer cells to find new environment where at least initially the nutrients an the space are very abundant. The acquisition of this new capability is characterized from complex processes which are not yet completely understood. However, they are often associated with at least one other of the five capabilities above described, involving both changes of the microenvironment and activation of extracellular proteases. Several classes of proteins are altered in cells bearing invasive and metastatic abilities, including cell-cell adhesion molecules (CAMs), calcium-dependent cadherin families, which mediate cell-to-cell adhesion and integrins, which link cells to the extracellular matrix substrates.[24]

Moreover, many lines of evidence have indicated the upregulation of extracellular proteases and the downregulation of their inhibitors as alternative strategy for the cancer cells to achieve invasive and metastatic capability.[25] Modifications of the functions or expression of the extracellular proteases can play a role also in other hallmark capabilities like angiogenesis[26] and growth signaling.[27]

2. EPIGENIC REGULATION

The understanding of the processes responsible for the acquisition of the enumerated six capabilities suggested that multiple changes in the genomes of cancer cells are required for their manifestation. The genome instability underlying all the processes above described is characterized from the malfunction of specific components of the system that monitors and repairs the DNA. Growing evidence suggests that the disruption of the epigenic events could represent a novel pathway for the onset and progression of cancer.[28] In fact, dynamic chromatin remodeling has been correlated with many DNA-templated biological processes, including gene transcription; DNA replication and repair; chromosome condensation; and segregation and apoptosis.[29]

DNA is conserved in a condensed and densely packed structure named chromatin. Chromatin is composed of regular repeating units of nucleosomes, which are complex of 146 nucleotide base pairs of DNA wrapped around the core histone octamer. The histone octamer is constituted of two copies each of H2A, H2B, H3 and H4 proteins, which can interact with DNA through the charged amino-side chains of amino acids like Lys and Arg, mainly localized in the N-terminal tail-region (Figure 2). The dynamic changes of chromatin are achieved through structural modification of histones (ATP-dependent

12

complexes, covalent histone modifications), utilization of histone variants and structural variation of the DNA (DNA-methylation).[30]
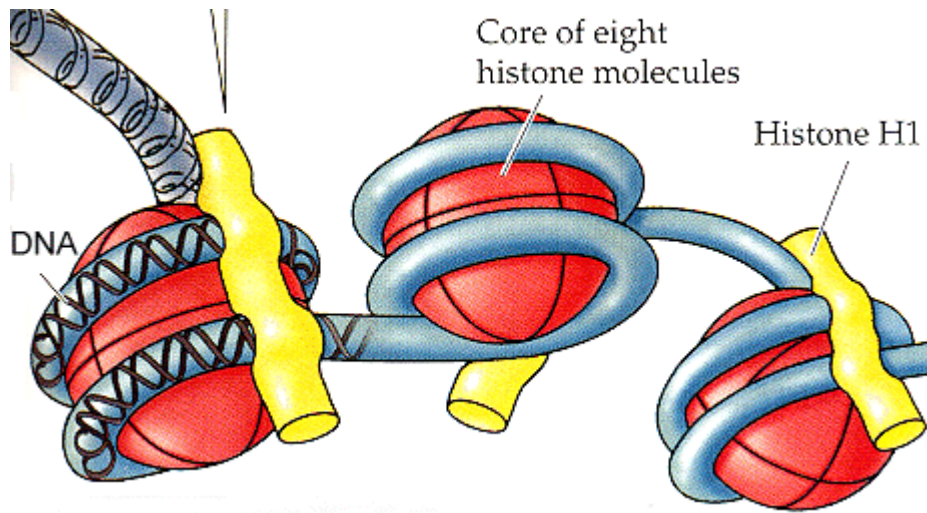
Figure 2. Nucleosome structure

2.1 Covalent histone modifications.

The covalent histone modifications are classified in eight different classes including lysine acetylation, lysine and arginine methylation, serine and threonine phosphorylation, lysine ubiquitylation, glutamate poly-ADP ribosylation, lysine sumoylation, arginine deimination and proline isomerization (Figure 3).[31]

The variety of molecular mechanisms underling the single covalent modification can be broadly generalized in two categories, *"cis"* mechanisms and *"trans"* mechanisms. *"Cis"* mechanisms produce alteration of intra- and internucleosomal contacts via changes of steric interactions. Prominent examples of the components

involved in these mechanisms are histone acetyltransferases (HAT) and histone deacetylases (HDACs), two families of enzymes that promote or repress the gene transcription by adding and removing acetyl groups from the side chains of Lys localized in specific position of the N-terminal region of histones.[32] *"Trans"* mechanisms involve the combination of specific histone modifications. First specific histone regions are modified by enzymes termed "writers" (e.g. histone methytransferase). Next, these modifications are recognized by second protein components of the system called "readers" (e.g. inhibitor of growth proteins, heterochromatin protein 1 and polycomb proteins) that translate the signal in the activation or repression of the transcription. Finally, when the signal is not anymore required it is removed by some other enzymes termed "erasers" (e.g. the jumonji, AT-rich interactive domain 1 demethylases).[33]

In addition, cross talking between existing histone modifications within the same histone tail or among different histone tails introduce another level of complexity in chromatin remodeling.[31]

Recently, a noteworthy correlation between loss of function of some components involved in the histone covalent modifications and tumorigenesis have been disclosed, providing the rationale for the development of alternative strategies for the treatment of tumors.
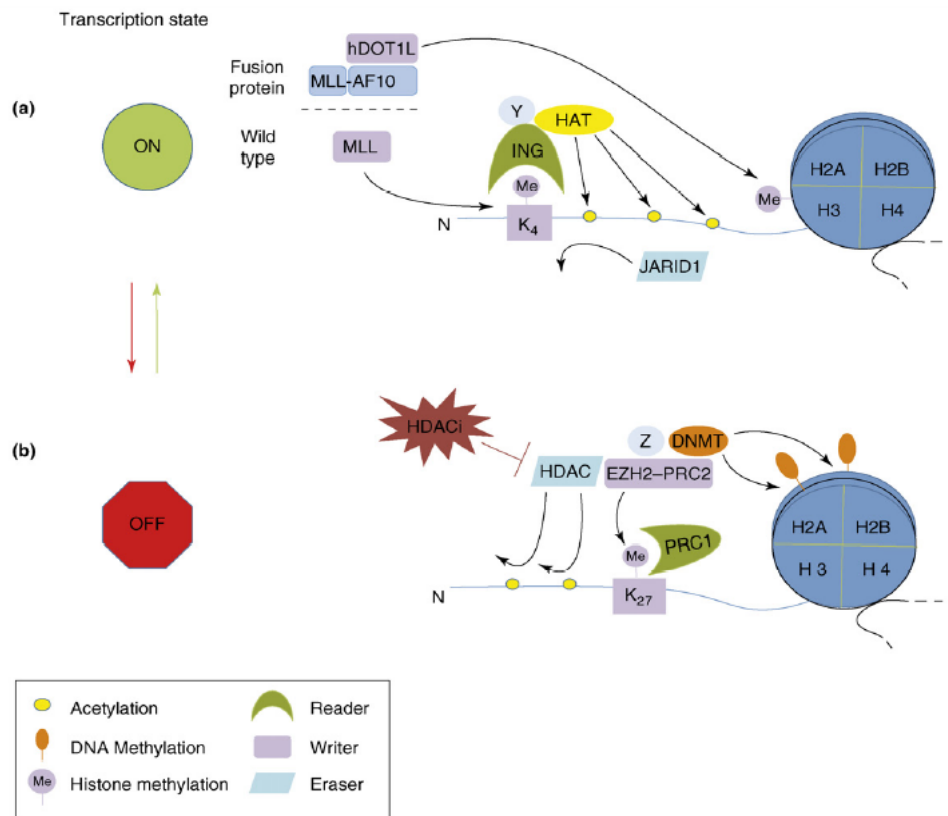
Figure 3. Dynamic changes of chromatin

2.2 Histone Lysine acetylation.

The acetylation state of the N^{ε} of Lys present in N-teminal tails of histones has been traditionally related with the modulation of the transcriptions events and with many other cellular functions including DNA replication and repair. Although transcriptional regulation is highly complex and dynamic, in general an increase level in histone acetylation causes remodeling of chromatin from a tightly packed configuration to a loosely packed configuration, which subsequently leads to transcriptional activation. On the other side, a decrease in histone acetylation cause the stabilization of condensed chromatin resulting in transcriptional silencing. Many lines of evidence have indicated the

inappropriate silencing of critical genes like tumor suppressor genes as one of mechanisms that could promote the tumorogenesis process.[34]

In addition to modification of histone, many non-histone cellular proteins like p53, pRb, E2F and Hsp90 undergo acetylation regulation, which mediate their involvement in diverse biological functions.[35] A relevant example is the p53 protein that loses its capability to monitor an correct potential genomic damages when inactivated by the deacetylation of the Lys localized in specific regions. Levels of acetylation of histone and non-histone proteins HDACs depend on the activities of two families of enzymes, histone acetylases (HATs) and histone deacetylases (HDACs) which add or remove acetyl groups from the protein substrates, respectively.
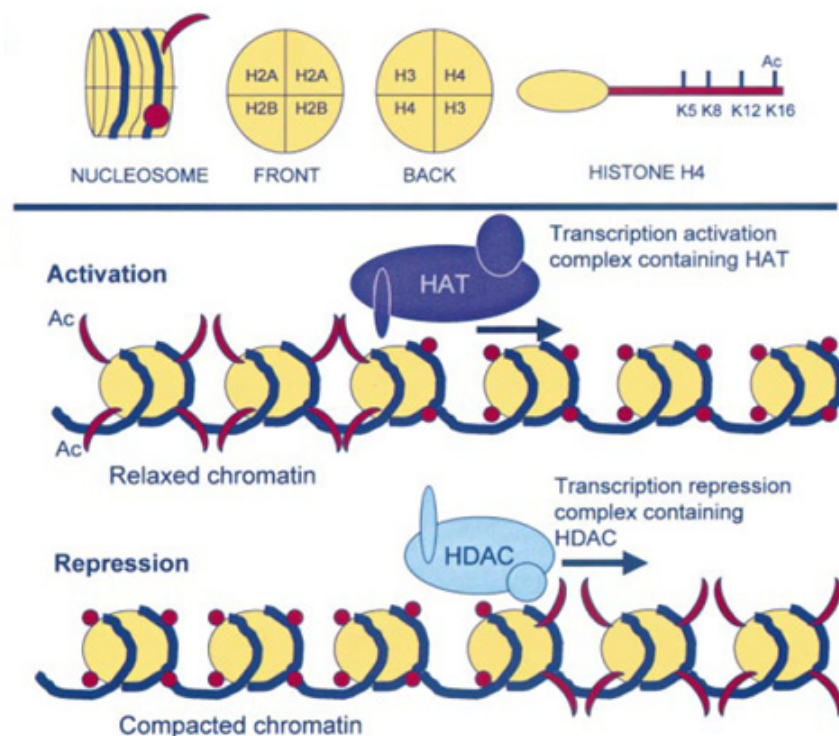
Figure 4. Histone lysine acetylation

There are three known families of HATs, the Gcn5-related N-acetyl transferase (GNAT) family, the MOZ/YBF2/SAS2/TIP60 (MYST) family andtheCBP/p300family.[36]They operate in forms of multisubunit complex acetylating with poor specificity multiple lysine sites in the core histones, which results in release of DNA promoting active transcription. Moreover, HATs acetylate several non-histone proteins such as p53, E2F and Hsp90 modulating their transcription activities on target genes.[51] Several studies support the connection between HATs deregulation and oncogenesis, demonstrating that aberrant localization or activation of HATs as well as its inactivation can origin oncogenic process.[36]

HDAC enzymes remove the acetyl group from the histones comprising the nucleosome. Hypoacetylation results in a decrease in the space between the nucleosome and the DNA that is wrapped around it. Tighter wrapping of the DNA diminishes accessibility for transcription factors, leading to transcriptional repression.

2.3 HDACs classification.

The 18 human HDACs identified at date have been categorized into four classes based on their homology with distinct yeast HDACs (Figure 5). Class III HDACs is an evolutionary distinct family of sirtuine (silent information regulators), that remove the acetyl group by a unique enzymatic mechanism dependent on the cofactor NAD^+. Class I, II and IV HDACs catalyze the deacetylation of histones in cooperation with a Zinc atom which is localized in the bottom of an enzyme pocket.
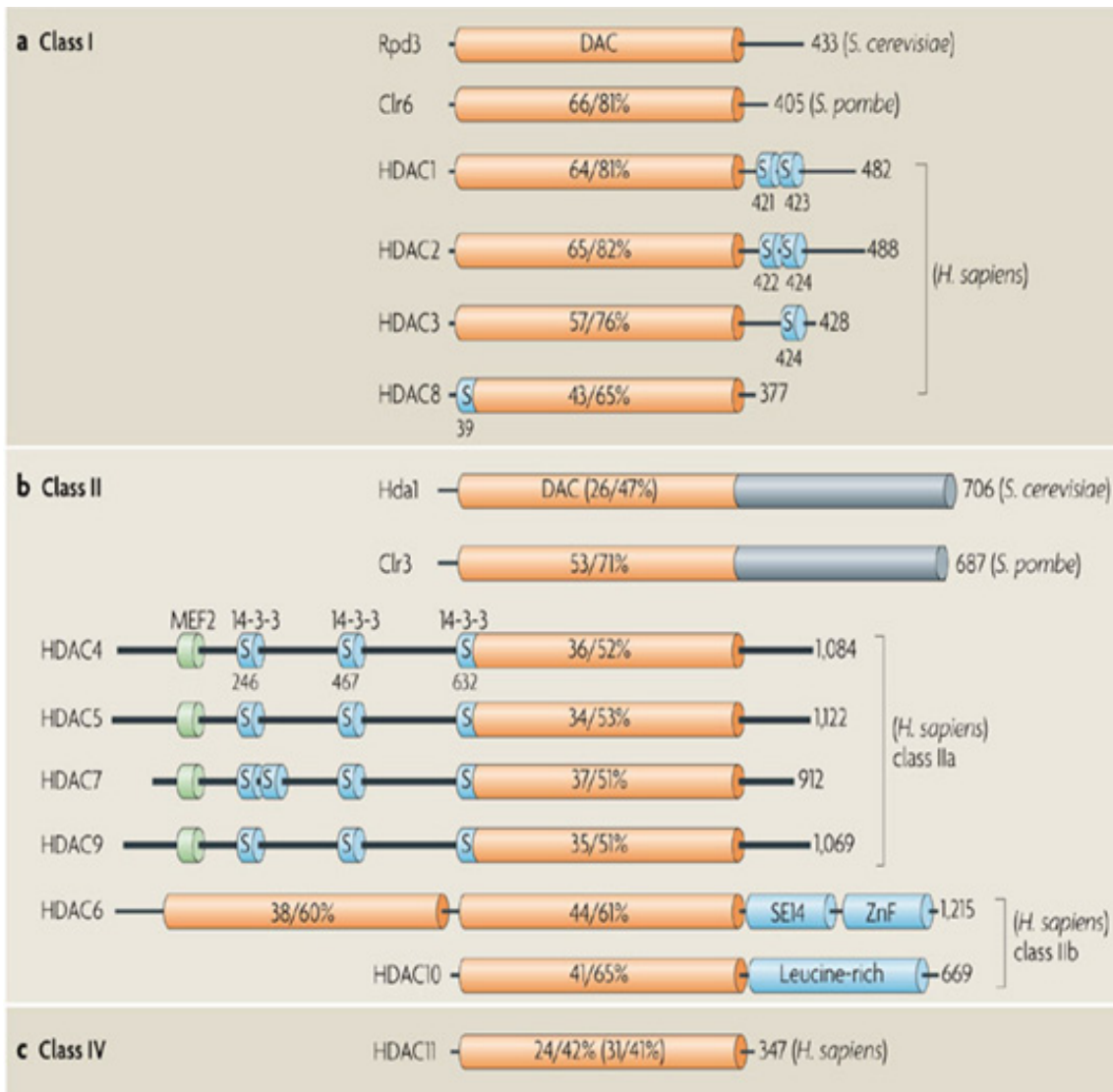
Figure 5. HDACs classification

2.3.1 Class I (HDAC 1, 2, 3, 8)

The members of this class present homology with the yeast Rpd1. HDAC I and II are exclusively localized in the nucleus, because of the lack of the nuclear exporting signal (NES).[37] HDAC 3 has both a nuclear import signal (NIS) and NES suggesting that despite it has been mainly found in the nucleus HDAC 3 can also localize in the cytoplasm. The nucleus localization of HDAC 3 could be explained by its recruitment by

HDACs 4, 5, 7 (Class II) when they are bound to DNA via co-repressors.[38] HDAC 8, is mainly found in the nucleus, but respect to the other HDAC enzymatic subtypes belonging to class I, it needed to be overexpressed to be localized because of its normal low abundance.[39] HDAC 1 and 2 (482 and 488 aa) are highly similar enzymes with an overall sequence identity of 82%. The catalytic domain is present on the N-terminal region and represents the major part of the enzymes. When produced by recombinant techniques *in vitro*, HDAC 1 and 2 are inactive suggesting the necessity of the presence of co-factors that form complex with them to restore the HDAC activity. In addition both the activity and complex formation are further regulated by phosphorylation.[40] HDAC 3 (428 aa) is most similar to HDAC 8 (with 34% overall sequence identity) and has N-terminal localization of the catalytic domain as all class I HDACs. In addition to the NLS that the other class I HDACs posses, a NES is also present in HDAC 3 (region 188-313). Apart from its capability to deacetylase the histones, studies performed *in vitro* and *in vivo* have demonstrated that HDAC 3 can also regulate the activity of HDAC 4, 5, 7 forming oligomers with them through complex formation with SMRT (silencing mediator for retinoic acid and thyroid hormone receptors) and N-CoR (nuclear receptor co-repressor).[41]HDAC 8 (377 aa) consists largely of the catalytic domain with a NLS in the centre. It is not yet completely clear if the HDAC 8 activity is regulated by co-repressor complex of proteins. The few information about the exact localization of HDAC 8 in our hands revealed a varying degree of its expression in several tissue.[42]

2.3.2 Class IIa (HDAC 4, 5, 7, 9)

The members of this family present homology with the yeast Hda1. HDAC 4, 5, 7, 9 are able to shuttle in and out from the nucleus in response to certain cellular signals.[43] The shuttling of HDAC 4, 5 and 7 (1084, 1122 and 1215 aa) between nucleus and

cytoplasm have been studied extensively in differentiating muscle cells and described in a clear model.[44] In response to differentiating signals HDAC 4 is phosphorylated by Ca^{2+}/calmodulin-dependent kinase (CaMK), resulting in the export of HDAC 4 along with CRM1 (cellular export factor for proteins bearing a leucine-rich NES). Once in the cytoplasm the phosphorylated HDAC 4/CRM1 complex is recognized and bound from a 14-3-3 protein (a cytosolic anchor protein) which retains HDAC 4 in cytosol. After that terminal differentiation occurs HDAC 4 is released from 14-3-3 protein due to decrease of its phosphorylation state and can shuttle back to the nucleus.[45] HDAC 5 resides in the nucleus during the proliferation state and it shuttles from the nucleus to the cytoplasm during the differentiation events. The mechanism of HDAC 5 export can be mediated from the same components already described for HDAC 4 (CRM1/ CaMK/14-3-3), although, since HDAC5 also has a NES domain, it could not be confirmed that it is solely responsible for the transport of HDAC 5 out of the nucleus.[46] It follows that both HDAC4 and HDAC5 reside initially in the same compartment, but end up in the cytosol and the nucleus respectively. HDAC 7 has a high degree of homology with HDAC 5 except the lack of the NES domain. As already described for HDAC 5 also HDAC 7 can shuttle from the nucleus to the cytoplasm during the differentiating events depending on the presence of CaMK and 14-3-3 protein. All three HDACs have their catalytic domains on the C-terminal half of the protein, and the NLS is situated close to the N-terminus. The N-termini of HDAC 4, 5, 7 interact specifically and repress the myogenic transcription factor MEF2, which plays a crucial role as a DNA binding transcription factor, in muscle differentiation. When associated with HDAC, MEF2 is inhibited blocking muscle cell differentiation. CaMK dissociates of this complex by phosphorylating the HDAC restarting the muscle cell differentiation.[44] Alternatively, the activity of HDAC 4, 5 and 7

is also associated with the presence of HDAC 3.[47] Thus, the activity of HDAC 4, 5, 7 seems to be a link between DNA binding recruiters and HDAC3-containing HDAC complex.

HDAC 9 splice variants are considered as separate group related to HDAC 4, 5, 7 and localized in the nucleus or cytoplasm depending on the variants. The catalytic domain is located in the N-terminus region. There are three different splice variant of HDAC 9, which are HDAC 9a, HDAC 9b and HDRP/HDAC 9c (1011, 879 and 590 aa).[43]

HDRP/HDAC 9c lacks the catalytic domain and presents 50% homology with N-terminus region of HDAC 4 and 5. The loss of the catalytic domain is overcoming by the capability to recruit HDAC 3. In addition HDAC 9 is able to interact with MEF2, indicating that HDAC 9 could have an important role in muscle differentiation.[48]

2.3.3 Class IIb (HDAC 6 and 10).

HDAC 6 (1215 aa) is evolutionary most closely related to HDAC 10 (669 aa) (37% sequence identity) and presents low degree of homology with the other HDAC isoforms. HDAC 6 is mainly localized in the cytoplasm but can be found also in the nucleus in complex with HDAC11, while HDAC 10 has been found in both nucleus and cytoplasm.[49]

HDAC 6 represent a very unique enzyme within the HDAC family, because it contains to catalytic domains arranged in tandem, which are very similar to the catalytic domain of HDAC 9.[51] Another unique feature of HDAC 6 is the presence in the C-teminus region of a HUB domain, which is a signal for ubiquination, indicating that is enzyme is very highly degraded.[43] HDAC 6 functions also as tubulin deacetylase, regulating microtubule-dependent cell motility.[49]

HDAC 10 (669 aa) is the most recently identified isoform of the class IIa HDACs. It has a catalytic domain in N-terminal, a NES and a putative catalytic domain in C-terminus. HDAC 10 is found to interact with HDACs 1, 2, 3 and HDAC 4, 5, 7 indicating an is potential role as recruiter rather than deacetylase. However, when expressed alone HDAC 10 shows the capability to deacetylate the histones.[51]

2.3.4 Class IV (HDAC 11).

The HDAC 11 has been classified recently as member of the class IV HDAC. It is located mainly in the nucleus but also in cytoplasm as complex with HDAC 6. HDAC 11 appears more closely related to HDAC 3 and 8, presenting the catalytic domain situated at the N-teminus, with proven deacetylase activity that can be inhibited by trapoxin (HDAC inhibitor).[52]

2.3.5 Class III (Sir 1-7).

Actually seven distinct mammalian HDAC have been identified and classified as members of this families of enzymes based on their unique catalytic domain characterized by its requirement for nicotine adenine dinucleotide (NAD) as cofactor.[53] Moreover they present higher overall identity degree with the yeast Sir2. Sir 1, 2, 6 and 7 are mainly localized in the nucleus while Sir 3, 4 and 6 have been found more in the mitochondria. In eukaryotes, sirtuins regulate transcriptional repression, recombination, the cell division cycle, microtubule organization, and cellular responses to DNA-damaging agents. Sirtuins have also been implicated in regulating the molecular mechanisms of aging.[54]

2.4 HDACs and cancer.

Zn^{++}-dependent HDACs, class I (HDAC 1, 2, 3, 8), class IIa (HDAC 4, 5, 7, 9a, 9b and HDRP/HDAC 9c) and class II b (HDAC 6 and 10) have been extensively associated with oncogenesis, while only recent studies indicate that Class III (Sir T1-7) could be involved in cancer process as well. Since the aim of our study was the design and synthesis of analogues of FK228, a well known Zn^{++}-dependent HDACs inhibitor, herein we are going to focus our attention on the understanding of the connection of aberrant recruitment and expression of this family of enzymes with cancerogenesis.[29]

Most studies relating to the aberrant recruitment of HDACs have reported that HDACs can be physically associated with DNA-binding oncogenic fusion proteins resulting in repression of specific onco-suppressor genes.[55] Moreover HDACs can also interact with specific repressive transmission factors that are overexpressed in the tumoral cells, producing repression of the transcription of fundamental growth-regulatory components like *CDKN1A* (encoding p21WAF1/CIP1).[56]

In addition to aberrant recruitment of HDACs to specific loci, also altered expression of specific HDACs in several tumoral cells has been reported. For example, HDAC 1 is overexpressed in prostate,[57] gastric,[58] colon,[59] and breast carcinomas,[60] while HDAC 2 is overexpressed in colorectal,[61] cervical[62] and gastric cancer.[63] An increased expression of HDAC 3 and HDAC 6 has been observed in colon[60] and breast[64] cancer, respectively.

These evidences highlighted that HDACs-inhibition induces in transformed cells biological responses such as apoptosis, cell cycle inhibition and differentiation through the selective reactivation in tumor cells of silenced oncogenic transcriptional repressors.[65]

This preliminary assumption might be confirmed in part from the recent finding that only transformed cells are sensitive to HDAC inhibitors-induced apoptosis.[66]

Thus, the transformed cells seem to alter the epigenome in such way that otherwise-silenced genes can be activated by HDACi. It follows that the therapeutic effects of HDACi are not accomplished by reversing the aberrant transcription mediated by the transforming oncogene, but rather through the effects on the malignant epigenome that result in the tumor-specific induction of pro-apoptotic gene.

2.5 Biological effects of HDACs inhibition (effects on histonic proteins).

HDAC-inhibition represents an emerging strategy for intervention in oncology. HDACi are considered as multitarget drugs exhibiting a range of cellular effects, including differentiation, inhibition of proliferation and induction of apoptosis.

2.5.1 HDAC-induced apoptosis.

In vitro studies have demonstrated that the treatment with HDACi results in an apoptotic response of the tumor cell lines ten folds higher then normal cell lines.[67] Despite the relationship between treatment with HDACi and tumor cell death had been widely demonstrated, the pathways which are engaged to mediate this effect need to be still fully elucidated. In addition, it seems that the effects of HDACi can be cell-type-dependent, and there is growing evidence that structurally diverse HDACi can have different effects in the same cell type. This might be directly related to the selectively of the inhibitors toward specific HDAC enzymatic isoforms.[66]

Death-receptor (extrinsic) pathway. Many studies have hypothesized a transcriptional activation of death receptor family TNF and their ligands following HDAC1 treatment.[68]

However, the correlation between HDACi signal and death receptors remains still controversial. In fact, almost all the HDACi-death receptor studies have been performed *in vitro* using human tumour cell lines, while only limited information are available on the effective role of the death receptor pathway on the HDACi-response. Insinga and colleagues performed an *in vivo* study using PML–RAR transgenic mice that develop AML to try to address this ssue.[69] HDACi-induced expression of TRAIL and Fas in AML cells was suppressed *in vivo* using TRAIL- and Fas-selective small interfering RNA (siRNA), resulting in a 50% reduction in apoptosis following treatment of mice with valproic acid (VPA*)*. Despite these data provided more information on the potential dependence of HDACi activity from the death receptor pathway, this correlation remains still unsolved.

Mitochondrial (intrinsic) death pathway. The involvement of the mitochondrial apoptotic pathway in HDACi-mediated tumor cell death has been proposed from alarge number of independent studies. A prominent example supporting this hypothesis is represented from the primary B-cell lymphomas overexpressing BCL2 that are completely resistant to SAHA and LBH589. How HDACi trigger activation of the intrinsic apoptotic cascade is a major question that remains to be fully answered. Two main models have been reported to address this issue. 1) *Selective activation or induction of BH3-only proteins.* BH3-only proteins regulate the activation of intrinsic apoptotic pathway by interacting with pro-apoptotic factors (Bax and Bak) or anti-apoptotic BCL2 family proteins.[70] BH3-only proteins can be activated transcriptionally or through post-transcriptional modifications in response to HDACi treatment.[71] However, the member of the BH3-only proteins family more sensible to HDACi and how they are activate in response to these agents are currently undefined. 2) *Regulation of ROS*

production/activity. The regulation of ROS production and activity represents an alternative pathway proposed as mechanism of HDACi-induced apoptosis and to explain the tumour-selective killing activity of these agents. This observation is supportedfrom several studies that have highlighted suppression of apoptotic activity of HACi when the cells are in presence of free radical scavengers.[72] How the levels of free radical are elevated in the cells after HDACi treatment remains still to be fully elucidated.

2.5.2 Cell-cycle arrest.

Tumor cell-cycle arrest associated with induction of cellular differentiation was the first capability described for HDACi.[73] Except Tubacin,[74] which is HDAC6 specific inhibitor, all HDACi studied to date can induce cell-cycle arrest G_1/S, through the p53-independent induction of *CDKN1A* (encoding p21WAF1/CIP1), that promotes the hypophosphotylation of pRb.[75] CDKN1A down-stream events seem to be partially responsible of the G1 arrest observed; in fact, HDACi can also repress *cyclin A* and *D genes*, that contribute at the loss of CDK2 and CDK4 kinase activities and hypophosphotylation of pRb. In addition, two important genes involved in DNA synthesis, *CTP synthase* and *thymidilate synthetase*, are repressed following HDACi treatment contributing to G_1/S arrest.[76]Moreover, in response to HDACi treatment the cells can activate other potential growth inhibitory mechanisms including regulatory genes such as *GADD45* α and *GADD45* β65, and upregulation of TGFβ receptor signalling, leading to repression of *c-MYC* and cell-cycle arrest.[77]

Additionally, HDACi can also mediate G2/M-phase arrest by activating a G2-phase checkpoint, although this is a much rarer event than HDACi-induced G1 arrest. In

some cases, the loss of the G2-phase checkpoint can determine apoptotic sensitivity to HDACi.[78]

2.5.3 Tumour angiogenesis, metastasis and invasion.

HDACi have showed anti-angiogenic, anti-invasive and immunomodulatory activities in vitro and in vivo, that could contribute to the inhibition of tumor development and progression. The anti-angiogenic activity has been associated with the capability of HDACi to downregulate pro-angiogenic genes like vascular endothelial growth factor (*VEGF*), basic fibroblast growth factor (*bFGF*), hypoxia inducible factor-1α (*HIF1α*), angiopoietin, tunica intima endothelial kinase 2 (*TIE2*) and endothelial nitric oxide synthase (*eNOS*).[79] These mechanisms along with others such as downregulation of the expression of chemokine (C-X-C motif) receptor 4 (CXR4) or suppression of endothelial progenitor cell differentiation[80] evidence that HDACi suppress neovascularization through alteration of genes directly involved in angiogenesis.

The anti-metastatic effect following HDACi treatment might be achieved through transcriptional repression of matrix metalloproteinasis (MMPs) or upregulation of TIMP1, TIMP2 and RECK, which play crucial roles in the negative control of MMPs.[81]

Recent studies have highlighted also a potential role of HDACi during the antitumor immunity response either by directly affecting malignant cells in order to make them more attractive targets or by altering immune cells activity and/or cytokine production. One of the proposed mechanisms is that HDACi can augment the immunogenicity of tumor cells by upregulating the expression of major histocompatibility complex (MHC) class I and II proteins and co-stimulatory/adhesion molecules like CD40, CD80, CD86 and intracellular adhesion molecule 1 (ICAM1).[82] Moreover, it has been

demonstrated that HDACi can also stimulate the expression on the surface of the tumor cells of MICA and MICB, two MHC class I chain-related molecules which interact with the activating immunoreceptor NKG2D (natural killer cell protein group 2D) presents on the surface of killer cells γδ T cells and CD8 T.[83]

As mentioned above the alternative strategy for HDACi to achieve immunomodulatory effects is by enhancing the immune responses through the directly or indirectly variation of cytokine secretion which results in alteration of the activities of immune cells.[84] At the present it is unclear whether this variation is closely correlated with the hypeacetylation of histones within the promoter/enhancer regions of cytokine genes or with other effects of HDACi.

2.6 Biological effects of HDACs inhibition (effects on non-histonic proteins)

The anti-cancer effects of HDACi above described are mainly correlated to their capability to regulate gene expression through the stabilization of hyperacetylated histones. However, histones are not the only molecular targets of HDACs, and therefore HDACi can affect tumor cell biology through pathways that do not directly involve histones.[85]

HDACi-induced apoptosis through "indirect" regulation of gene expression. Increasing evidences indicate that HDACi-mediated gene expression is not necessarily correlated only with the acetylating state of histones but rather also with the regulation of transcription factors such as E2F1, p53, STAT1, STAT3 and NF-κB.[86] It has been observed that the hyperacetylation of these proteins in response to HDACi can affect the

expression of downstream target genes, not through direct promoter hyperacetylation of these genes, but through the activity of the hyperacetylated transcription factors. Moreover, recent studies support a role for acetylation of transcription factors in mediating the selective induction of apoptotic genes in response to DNA damage. For example, although several studies have demonstrated that expression of wild type p53 is not necessary for the HDACi-induced apoptosis, these agents can regulate the activity of both wild and mutated p53 to induce a p53-mediated apoptosis.[87] The activation of p53 results in a transcriptional induction of pro-apoptotic genes including Bax, the BH3-only genes Puma and Noxa, and in a functional repression of anti-apoptotic factors such Bax, BCL-XI and BCL2, which are directly bound by p53.[88] Together, these p53-mediated responses initiate a strong apoptotic signals. The stabilization of the hyperacetylated form of wild-type p53 increases the expression of p53 target genes such as those above mentioned to start the apoptosis.[89]

Intriguingly, recent evidences have reported the capability of HDACi to induce the specific degradation of mutant p53 through strong induction of the wild-type p53 activity induced by mutant p53.[90]

In some instances it has been observed that the hyperacetylation and activation of transcriptional factors can prolong cell survival instead than cell death. This could be the case for the NF-κB protein p65/RelA, that, when hyperacetylated can not be sequestered by inhibitor and NF-kB and can translocate to the nucleus where it is involved in the activation of anti-apoptotic genes including X-linked inhibitor of apoptosis (*XIAP*) and *BCL-X$_L$*.[91]

HDACi-induced apoptosis independent of altered gene expression. Although most of the biological effects such as apoptosis and cell cycle arrest of HDACi have been correlated with direct and indirect regulation of transcriptional factors, it is probable transcription-independent effects of HDACi are also important in their anticancer activities.[92] For example, while the hypoacetylated form of the DNA end-joining protein Ku70 binds to and sequester Bax in the cytoplasm, acetylation of Ku70 in response to HDACi releases Bax, which can interact with mitochondrial membrane initiating apoptosis.[93]

In addition HDACi have showed the capability to affect the activity of diverse kinase-mediated signal transduction pathways resulting in dysregulated phosphorylation of various downstream substrates. For example, HDAC 6, protein phosphatase PP1, and α-tubulin form a complex that once disrupted by HDACi results in α-tubulin hyperacetylation and microtubule stabilization.[94]

Recently, it has been highlighted also a potential involvement of HDACs in the regulation of the activity of heat-shock protein 90 (Hsp90), which is an abundant chaperone whose overexpression in tumor cells and correlates with poor prognosis and resistance to chemotherapy.[95] Inhibition of HDAC6 induce hyperacetylation of Hsp90, which leads to the proteasomal degradation of Hsp90 client proteins HER2/*neu*, ERBB1, ERBB2, Akt, c-Raf, BCR-ABL and FLT3. The importance of hyperacetylation of proteins such as Hsp90 and α-tubulin as major mediator of HDACi-induced apoptosis remains to be determined.[96]

3. HDAC INHIBITORS

Until now, many inhibitors of Class I, II and IV HDACs have been isolated from natural source or synthetically developed. HDACi cause cell cycle arrest and/or apoptosis of many tumors by blocking the access of hostone and non histone substrates to the enzyme catalytic pocket. With few exceptions, HDACi can be divided in six different classes based on their chemical features,[97] including:

1.   *Short-chain fatty acids such as valproic acid (VPA) and butyric acid*

2.   *Hydroxamates such as Trichostatin A (TSA), Suberoylanilide hydroxamic acids (SAHA)*

3.   *Benzamides such as MS-275 and CI-994*

4.   *Cyclic peptides such as FK228, Trapoxin A, Apidicin and CHAPs*

5.   *Electrophilic ketones (Triluoromethylketone),*

6.   *Other hybrids compounds such as Depudecin and MGCD-0103*

The first known member of HDACi is the butyrate which was proposed to have anticancer activities based on its capability to induce cellular differentiation. Only in 1990, the suppression of tumor cell growth/survival following butyrate treatment was linked with the inhibition of HDACs activity.[98]

Several HDACi are currently in phase I/II clinical trials both in hematological malignancies and in solid tumors. Compared with agents used initially which were active

at millimolar or micromolar concentrations, some newer agents such as FK228 and TSA
are effective at nanomolar concentrations and are relatively less toxic.

Despite the wide range of structures, most of these HDACs inhibitors can be
broadly characterized by a common pharmacophore that consists in a hydrophobic cap
that blocks the access to the active site (1) connected by a spacer (2) to a functional zinc-
binding group (ZBG) (3) (Figure 6).[99]
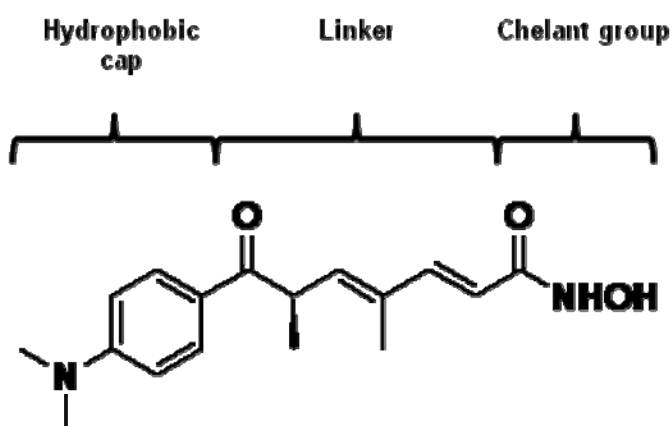
Figure 6. Pharmacophore model for HDACi-TSA

The different ZBGs (carboxylate, hydroxamate, sulfhydrilic and ketone) interact
with the Zn^{++} ion located in the bottom of a tunnel (11 A deep in HDLP) completing
along with two aspartates and one histidine the coordinator sphere of the metal. The
channel accommodates the linker region of the ligand and provide additional stabilization
through hydrophobic interaction. The cap region of the different HDACi can be oriented
toward several distinct pockets in the solvent-exposed entrance of the channel that are less
conserved across the different HDAC isoforms (Figure 7).
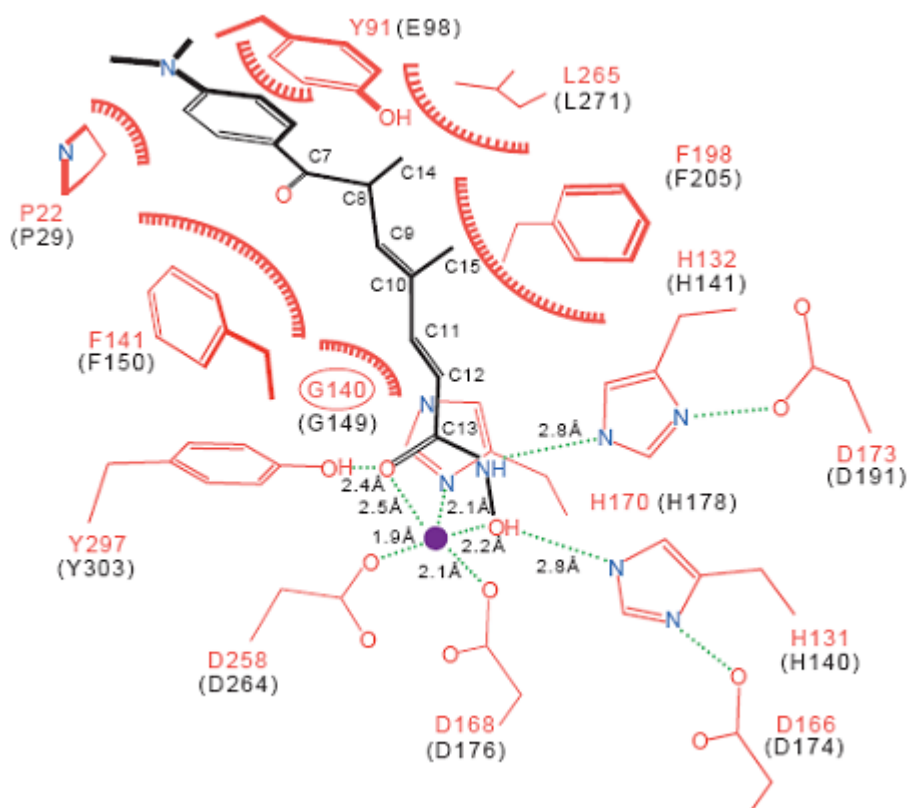
Figure7. Proposed model of interaction of TSA with HDAC active-pocket.

Although most of HDACi under investigation were not developed to be selective inhibitors of individual HDAC subtypes, it remains still a challenge to develop selective inhibitors which could be useful to achieve more information about the underlying biochemical processes involved in the cancerogenesis.[100]

Among those under pre-clinical investigation, FK228 (also known as FR901228 or Romidepsin) is a natural product isolated from *Chromobacterium Violaceum* (Figure 8).[101] It is structurally unrelated to the other HDAC inhibitors bearing a unique bicyclic depsipeptide which works as stable prodrug (Figure 8). As Furumai *et al.* have demonstrated, FK228 becomes activated by the reduction of its disulfide bond after uptake into cells releasing a sulfidryl group that appears to be important for the

interaction with the Zinc cation located at the bottom of the active site.[102] In addition, it shows high selectivity toward class I HDACs,[103] which seems to be mainly relevant for therapeutic intervention in oncology.[104]
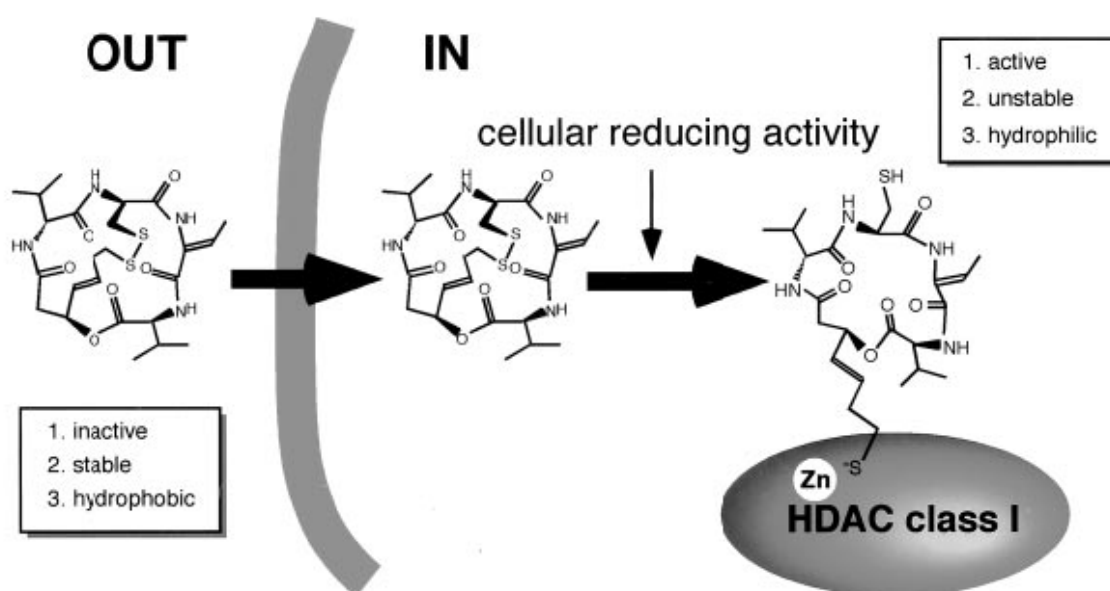
Figure 8. FK228 structure and its proposed mechanism of activation into the cell

Despite its exceptional activity, no significant derivatizations have been performed on FK228 mainly due to its synthetic difficulties, which were highlighted from Simon and co-workers that first reported its synthesis (18% overall yield in 16 steps[105]).

Very recently, an improved synthetic route has appeared, in which the heptenoic acid was build using an asymmetric Noyori hydrogen transfer reaction, however no increase in overall yield (13%) was achieved.[106]

In both the studies, three principal challenges associated with the synthesis of the byciclic depsipeptide structure were noticed, that are (1) the asymmetric synthesis of the

(*3S,4E*)-3-hydroxy-7-mercapto-4-heptenoic acid; (2) the macrolactonization to form the 16-membered cyclic depsipeptide; and (3) the oxidation of thiols to form the 15-membered ring.

4. RESULTS AND DISCUSSION

4.1 Design.

To overcome the synthetic difficulties identified from the previous synthesis,[105-106] the most synthetic challenging moiety (3*S*,4*E*)-3-hydroxy-7-mercapto-4-heptenoic acid in FK228 was modified into a structure that can be easily assembled using readily available starting materials, yet still has a capability to retain the same conformation required for the biological activity.[107]

First, the trans double bond in the heptenoic acid was replaced by an isosteric amide bond. Often, to develop peptidomimetics, an amide bond in peptides has been successfully replaced with a trans double bond because of its structural rigidity and capability to present two alkyl chains on opposite sides.[108]

Second, the ester bond to form the depsipeptide was replaced by another amide bond for facile ring closure that can provide higher synthetic yield and increased in vivo stability.[109]

These two simple modifications transformed the synthetically challenging heptenoic acid into (S)-3-Amino-4-(2-mercaptoethylamino)-4-oxobutanoic acid, a structure that can be easily assembled with an L-aspartic acid and a cysteamine (Figure 9).
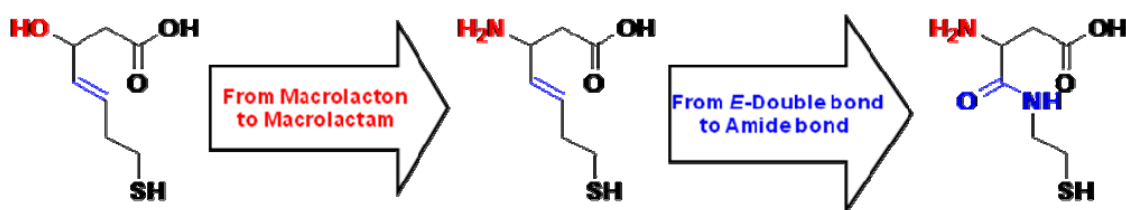
Figure 9. From (3E,4S)-3-hydroxy-7-mercapto-4-heptenoic acid to S)-3-Amino-4-(2-mercaptoethylamino)-4-oxobutanoic acid.

To assure similar structures between FK228, the novel FK228 analogue bearing a *L*-Ala at position originally occupied by *Z*-Dhb was examined by molecular modeling. A Monte Carlo conformational search using MacroModel[110] (version 9.1, Schrödinger) and united atom AMBER force field, showed the almost identical structure compared to FK228 (RMSD = 0.20 Å; Fig. 1B). Thus, the isosteric replacement of (*3S,4E*)-3-hydroxy-7-mercapto-4-heptenoic acid with (S)-3-(2-mercaptoethylcarbamoyl)-3-aminopropanoic acid appeared to not alter significantly the original backbone structure of FK228 (Figure 10).
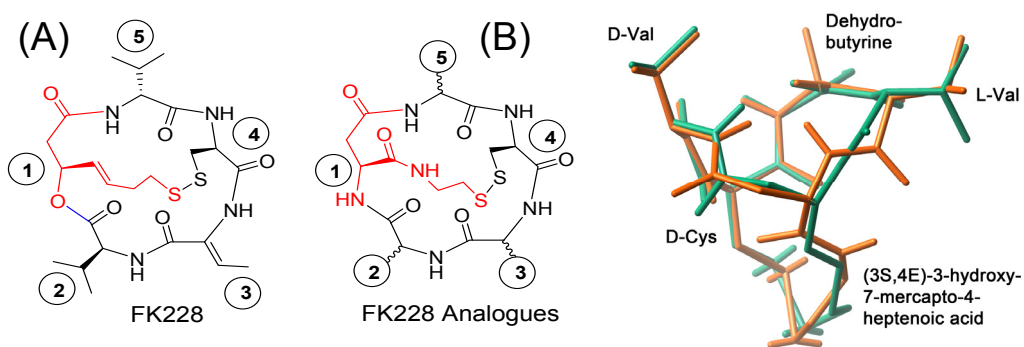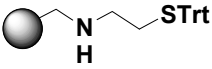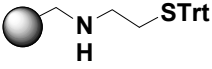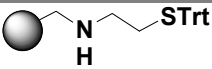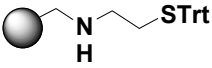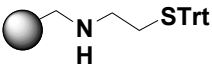

Figure 10. Structures of a novel FK228 analogue. (A) Analogue design and (B) conformation (orange) overlaid on FK228 (green).

4.2 Synthesis.

All the 62 compounds (**1-62**) have been synthesized adopting a high efficient solid-phase synthetic route, which we have developed and reported in the first part of our study as platform for the production of a large number of compounds.[107] Subsequently, five generations of compounds were prepared (Figure 2-6), wherein in addition to the introduction of the aspartilcysteamine moiety, the first two primary involved the incorporation of variegate amino acids to the positions occupied by *L*-Val and *Z*-Dhb in the original FK228 structure. The biological results achieved from the preliminary screening of the first series of analogues inspired the design of the other successive three series of compounds.

As shown in **scheme 1**, the FK228 analogues were synthesized anchoring a cysteamine by reductive amination on an Aminomethylated-Polystyrene (AM-PS) resin previously functionalized with a backbone amide linker (BAL linker).[111] To the resulting secondary amine (**1**), the first amino acid, Fmoc-L-Asp(OAl), was coupled with HBTU[112] for 12 h (80% yield). However, when several coupling methods were screened (see Table 1), TFFH[113] was found to provide a higher yield (95%). Also, coupling the amino acid as a symmetric anhydride by treating with DIC was effective (98% yield). Thus, the aspartylcysteamine (**2**) was constructed by one simple coupling reaction and represents a surrogate for the challenging heptenoic acid that was synthesized over five steps (51% yield) in the previously reported synthesis.

Table 1. Conditions for the coupling of Aspartic acid.

RESIN	AA$_1$	CC$_2$	t (h)	YIELD
(resin)—N(H)—STrt	Fmoc-Asp(OAll)-OH (4 eq)	HBTU/HOBt/DIEA (4:4:8 eq)	12	80%
(resin)—N(H)—STrt	Fmoc-Asp(OAll)-OH (4 eq)	Bop/HOBt/DIEA (4:4:8 eq)	12	85%
(resin)—N(H)—STrt	Fmoc-Asp(OAll)-OH (4 eq)	PyBrop/DIEA (4:4 eq)	12	88%
(resin)—N(H)—STrt	Fmoc-Asp(OAll)-OH (4 eq)	TFFH/DIEA (10:10 eq)	12	95%
(resin)—N(H)—STrt	Fmoc-Asp(OAll)-OH (10 eq)	DIC/DIEA (5:5 eq)	12	98%
(resin)—N(H)—STrt	Fmoc-Asp(OAll)-OH (4 eq)	DIC/DIEA (2:2 eq)	12	98%

The remaining four amino acids required to build a linear pentapeptide were introduced using standard *N*-Fmoc/^{t}Bu solid-phase peptide synthesis strategy (**64-68**). For the construction of the bicyclic structures, the *D*-Cys was conserved in all FK228 analogues. All reactions used to prepare linear pentapeptides (**68**) proceeded with high yields and high purity (> 95%).

The allyl protecting group of the linear pentapeptides (**68**) was selectively removed, followed by the deprotection of the *N*-Fmoc group and then the macrolactam (**69**) was formed by treating with a coupling reagent like HBTU for 3 h with high purity (> 95%).

Next, the Trt protecting groups was selectively removed by TFA (1% in DCM), and the resulting free thiols were oxidized using iodine to make a disulfide bond. The bicyclic FK228 analogue (**1-62**) was cleaved from the resin by TFA (95%) and characterized by HPLC and ESI-MS. The synthetic scheme developed revealed to be very powerful providing high overall yield (75-90%) and purity (80-94%) for all the compounds herein described.

Scheme 1. Synthesis of FK228 analogues[a]
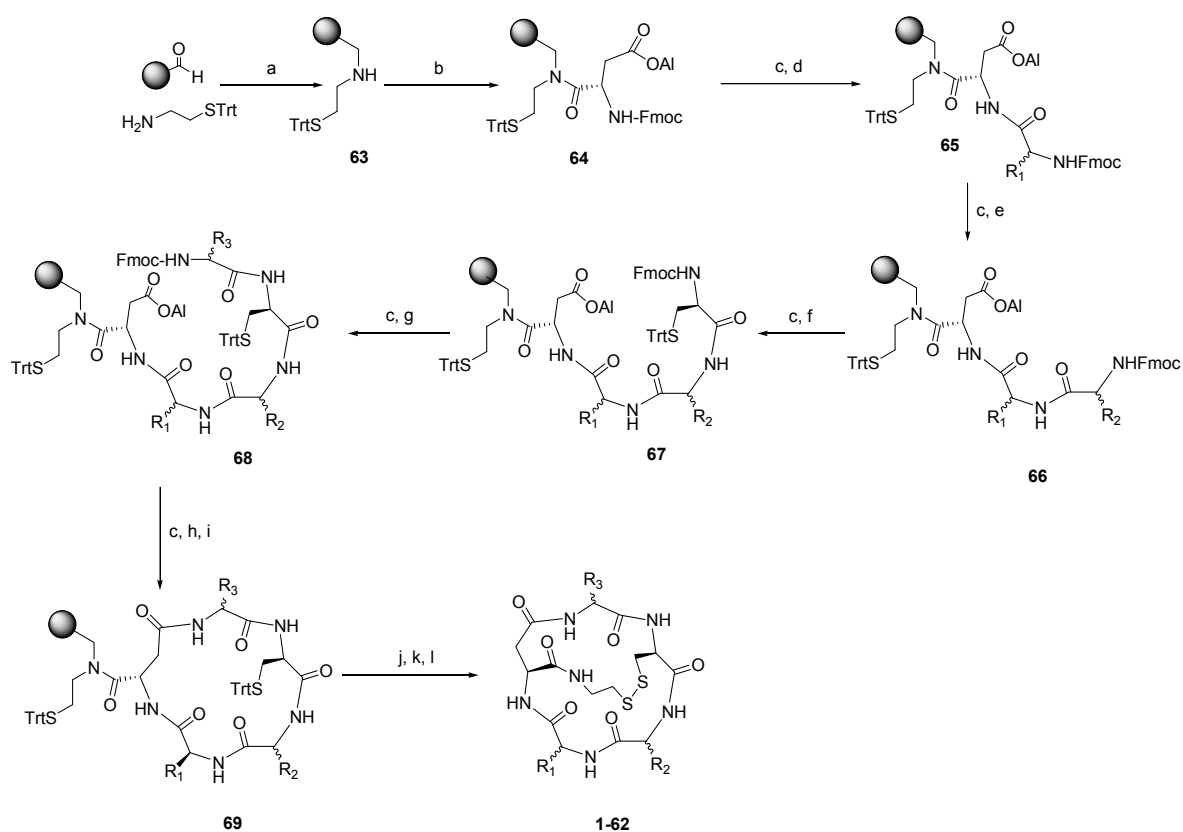
[a]Reagents and conditions. (a) NaBH$_3$CN; (b) Fmoc-Asp(OAl),DIC; (c) Piperidine; (d) Fmoc-AA$_1$, HBTU; (e) Fmoc-AA$_2$, HBTU; (f) Fmoc-D-Cys(Trt), HBTU; (g) Fmoc-AA$_3$, HBTU; (h) Pd(PPh$_3$)$_4$, DMBA; (i) HBTU; (j) 1% TFA; (k) I$_2$; (l) TFA

To synthesize the analogues **1** and **34**, *Z*-Dhb was introduced in solid phase adapting the steps reported in the previous synthesis.[105]

A monocyclic peptide bearing *L*-Thr at the position of the *Z*-Dhb (**69**) was constructed as described above in the general scheme. Then, the β-hydroxyl group of the Thr was first tosylated and then eliminated by DBU treatment resulting in the introduction of *Z*-Dhb (**70**) as described in scheme 2. The formation of the tosylated intermediate and its successive dehydration were quantitative monitored by analytical HPLC.

Next, due to the presence of the α-β unsaturated system of *Z*-Dhb, the reaction conditions for formation of the disulphide bridge were investigated adopting also an alternative solution phase strategy in order to evaluate potential side reactions resulting from the iodine treatment.

Thus, first the disulphide bond was formed using iodine at similar reaction conditions described in scheme 1, and the bicyclic compound was finally removed from the resin using TFA (95%) and later characterized by HPLC and ESI-MS.

Alternatively, the solid phase synthesis was stopped after the formation of the *Z*-Dhb and the monocyclic compound **71** was cleaved from the resin, recovered and then oxidized to **1** in solution using milder oxidant reagent like DMSO for a time of 36-48 h.

Both the strategies for the conversion of the monocyclic intermediates **70** and **71** to **1** were monitored by HPLC and later confirmed by ESI-MS and resulted to be quantitative. Interestingly, no significative side products were noticed for the solid-phase oxidation with iodine, probably due to the short time of reaction which minimized the possibility of undesired reactions. Moreover, higher yields were observed with the solid phase strategy (75% Vs 60% yields), probably because of the work-up required to remove the DMSO from the solution, which resulted in a loss of material.

Scheme 2. Synthesis of *Z*-Dhb analogue in solid phase[a]
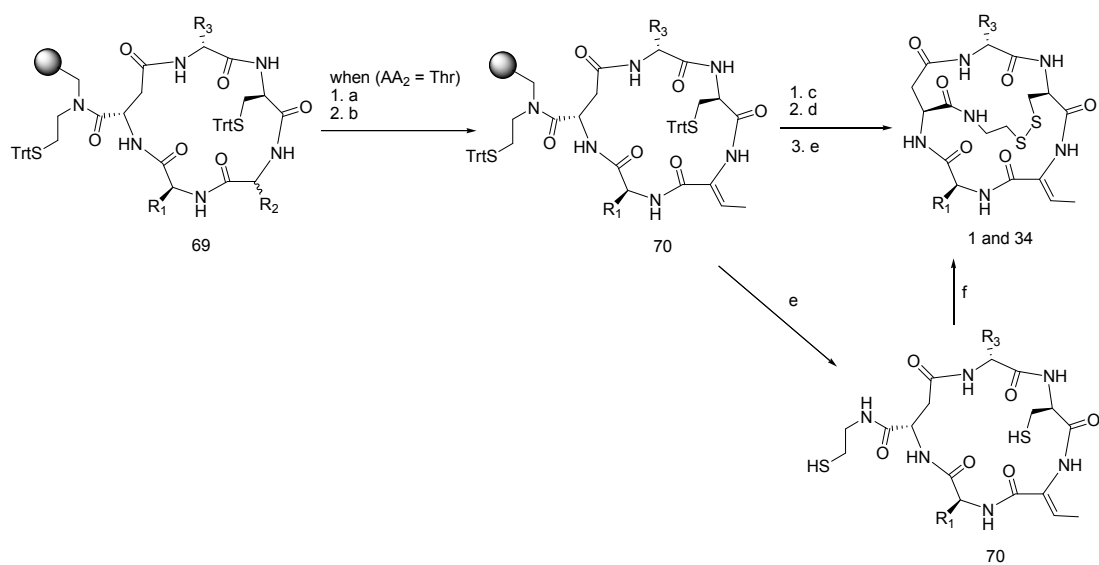
[a]Reagents and conditions. (a) Ts-Cl/Pyr; (b) DBU; (c) 1% TFA; (d) I_2, HBTU; (e) TFA; (f) DMSO/CH$_3$OH/H$_2$O/NaHCO$_3$

4.3 Antitumoral activity and Structure-activity relationship study (I part)

FK228 has been reported to strongly inhibit the growth of several human cancer cell lines, such as T24 cells derived from urinary bladder carcinoma.[114] To examine antitumoral activity, a total the 62 analogues synthesized were preliminary screened using T24 cells at the concentration of 0.5 and 5 μM. The potency exhibited by FK228 is shown so that comparisons can be made between the natural product and our synthetic analogues. The histogram for each series of compounds shows the percent of inhibition of growth produced by a concentration of 0.5 and 5 μM compound. Later, to further evaluate the efficacy of the active compounds identified, two of them were selected and assessed on six different cancer cell lines (prostate and bladder).

4.3.1 First series.

The compounds **1** was generated introducing the aspartilcysteamine moiety in the original amino-acidic sequence of the FK228 (*L*-Val-*Z*-Dhb-*D*-Cys-*D*-Val), while the first series of analogues was synthesized through the incorporation of variegate natural amino acids bearing aliphatic (*L*-Ala, *L*-Val, *L*-Leu, *L*-Ile, *L*-Pro), aromatic (*L*-Phe, *L*-Trp, *L*-His) and polar (*L*-Lys, *L*-Asp, *L*-Thr) side-chains at the position 3, which was occupied from a *Z*-Dhb in the original FK228. Moreover, the study of the third position was accomplished introducing unnatural amino acids such as *L*-Phg, Aib, *D*-Ala.

The growth inhibition data shown in the Figure 11 evidence that, surprisingly, no compound of this first generation provided satisfy activity (IC$_{50}$ > 100 µM, data not reported), whether the presence of *Z*-Dhb or not at position 2 (**1-15**). These results appeared to advise that the presence of the aspartilcysteamine moiety results in significative structural-changes that lead to a loss of potency no matter the nature and the stereochemistry of the amino-acids introduced at the position 3.

	R$_3$			R$_3$
1	*Z*-Dhb		8	*L*-Phe
2	*L*-Ala		9	*L*-Trp
3	*L*-Val		10	*L*-Lys
4	*L*-Ile		11	*L*-His
5	*L*-Leu		12	*L*-Asp
6	*L*-Pro		13	*L*-Thr
7	Gly		14	*L*-Nle
			15	*D*-Ala

Figure 11. I series of compounds

4.3.2 Second series.

Despite the discouraging results observed testing the first series of compounds, we proceeded with the synthesis of the second generation of compounds, which was created keeping the position 3 as *L*-Ala, while the position of *L*-Val was investigated with different *L*- and *D*- amino acids.

The choice to keep a *L*-Ala at position 3 in place of a *Z*-Dhb resulted from two main considerations:

1. No significant difference in terms of activity were observed between the compounds bearing *Z*-Dhb (**1**) and *L*-Ala (**2**) at the position 3.

2. The introduction of a *Z*-Dhb moiety required some more steps of reactions.

	R$_2$			R$_2$
16	*L*-Ile		**20**	*L*-Nle
17	*L*-Leu		**21**	*L*-Asp
18	*L*-Phe		**22**	*L*-Ala
19	*L*-Lys		**23**	*D*-Val
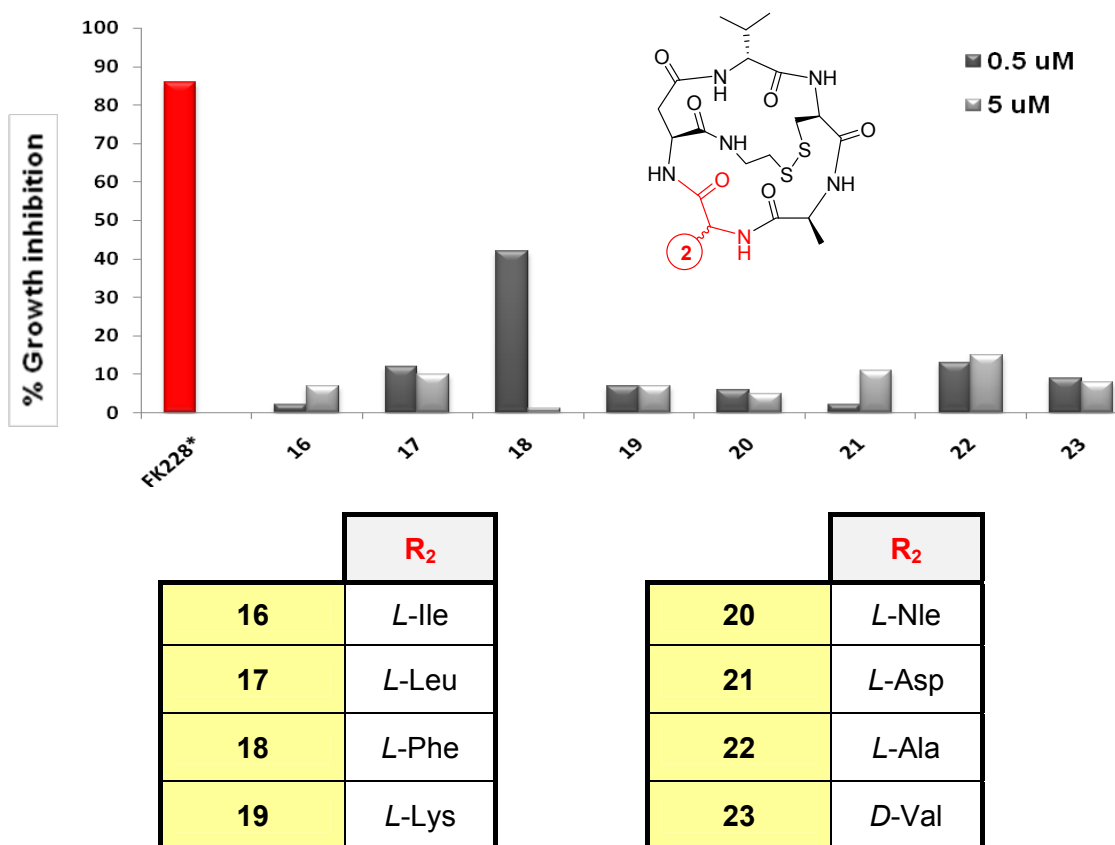
Figure 12. II series of compounds

As shown in Figure 12 only the compound **18** with a *L*-Phe at the position 2 produced 37 % cell growth inhibition at 5 μM while the other members of the series (**16, 17, 19, 20, 21, 22, 23**) containing respectively (*L*-Ile, *L*-Leu, *L*-Lys, *L*-Nle, *L*-Asp, *L*-Ala, *D*-Val,) at the position 2 were found to be inactive providing results in lane with those observed testing the first series of compounds.

Thus, almost all the compounds belonging to the first and second series did not provide any satisfy activity; however the introduction of an aromatic ring like L-Phe partially restored the cytotoxic activity leading to the compound **18** which is 1000-fold less potent than FK228.

4.3.3 Third series.

The compound **18** was selected as new lead compound to synthesize a new batch of analogues replacing the *L*-Ala in position 3.

As reported in the histogram in Figure 13, the introduction of polar like *L*-Lys and *L*-Asp at position 3 (**24** and **25**) appeared to be not tolerated resulting in a completely loss of activity. Conversely, the presence of bulkier aliphatic amino acids as *L*-Ile and *L*-Leu, resulted in compounds (**27** and **28**) at least twice more potent than **18**, while the analogue bearing the unnatural amino acid *L*-Nle at the position 3 (**29**) revealed to be about 10 times more potent than **18**. Moreover, when a *L*-Phe was introduced in place of a *L*-Ala (**26**) an additional increment of activity was observed leading to the most potent compound of the third series, which showed 99 % growth inhibition at 5 μM (70% growth inhibition at 0.5 μM).

Interestingly, the replacement of the *L*-Phe with different aromatic amino acids as *L*-Tyr and *L*-Trp produced a loss of activity. Also, a stereo chemical preference was

observed at the position of *Z*-Dhb, that when was substituted with a *D*-Phe resulted in a compound which was significant less potent than **26**.
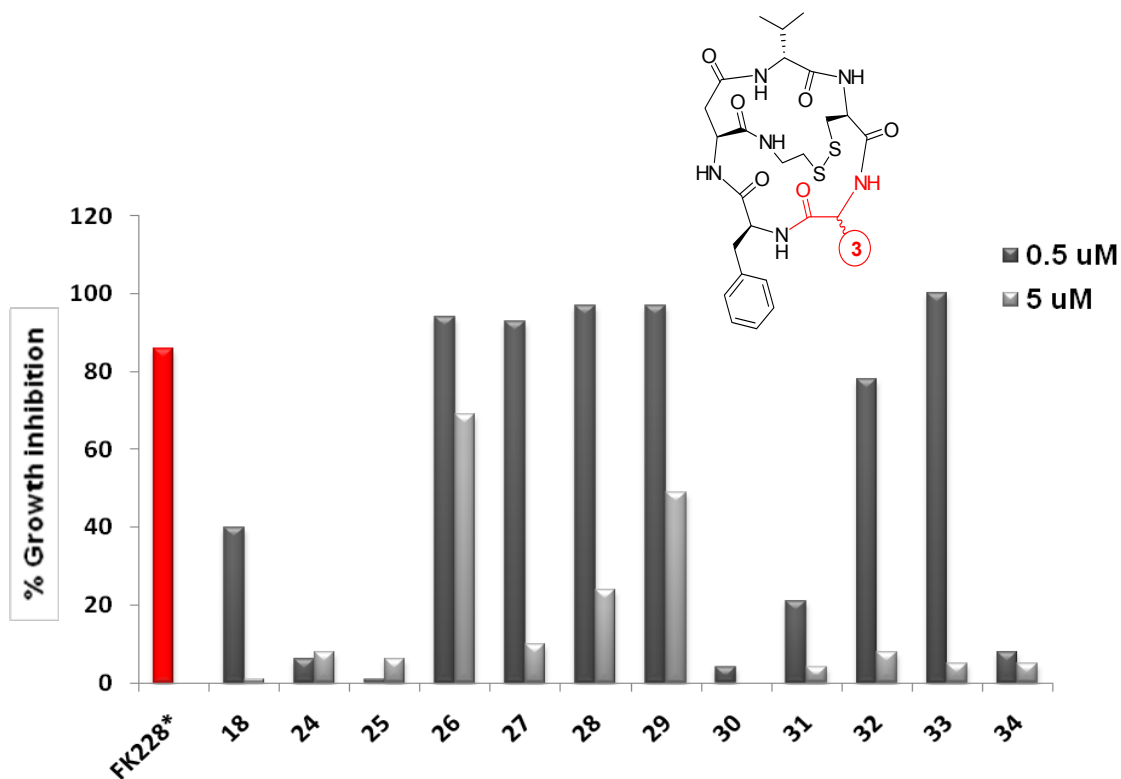
	R₃
18	*L*-Ala
24	*L*-Asp
25	*L*-Lys
26	*L*-Phe
27	*L*-Ile
28	*L*-Leu

	R₃
29	*L*-Nle
30	*L*-Pro
31	*L*-Tyr
32	*L*-Trp
33	*D*-Phe
34	*Z*-Dhb

Figure 12. III series of compounds.

The biological information achieved testing this third series of compounds let us formulate two important considerations. First, the enhancement of activity observed for

the compounds **27-29** provided more evidences that validated our hypothesis on the involvement of the aromatic ring in **18** in restoring the citotoxicity. Second, the further significative increment of cytotoxicity resulted from the introduction of a second *L*-Phe and subsequent decrease of activity following its replacement with amino acids bearing different aromatic side chains or stereochemistry, revealed additive important features of the position 3, such as stereo preference, important for the activity.

4.3.4 Fourth series.

The fourth generation of compounds was designed starting from **26** and replacing the position 5 originally occupied from a *D*-Val. First, the importance of the C^{α}-stereocenter with *D*-configuration at the position 5 was demonstrated synthesizing and testing the compounds bearing respectively an *L*-Val and Gly (**44** and **40**) in position 5, which were found to be remarkably less potent then **26** (Figure 5).

	R₅
26	*D*-Val
35	*D*-Ala
36	*D*-Leu
37	*D*-Ile
38	*D*-Nle
39	*D*-Pro

	R₅
40	Gly
41	Aib
42	*D*-Phe
43	*D*-Phg
44	*L*-Val
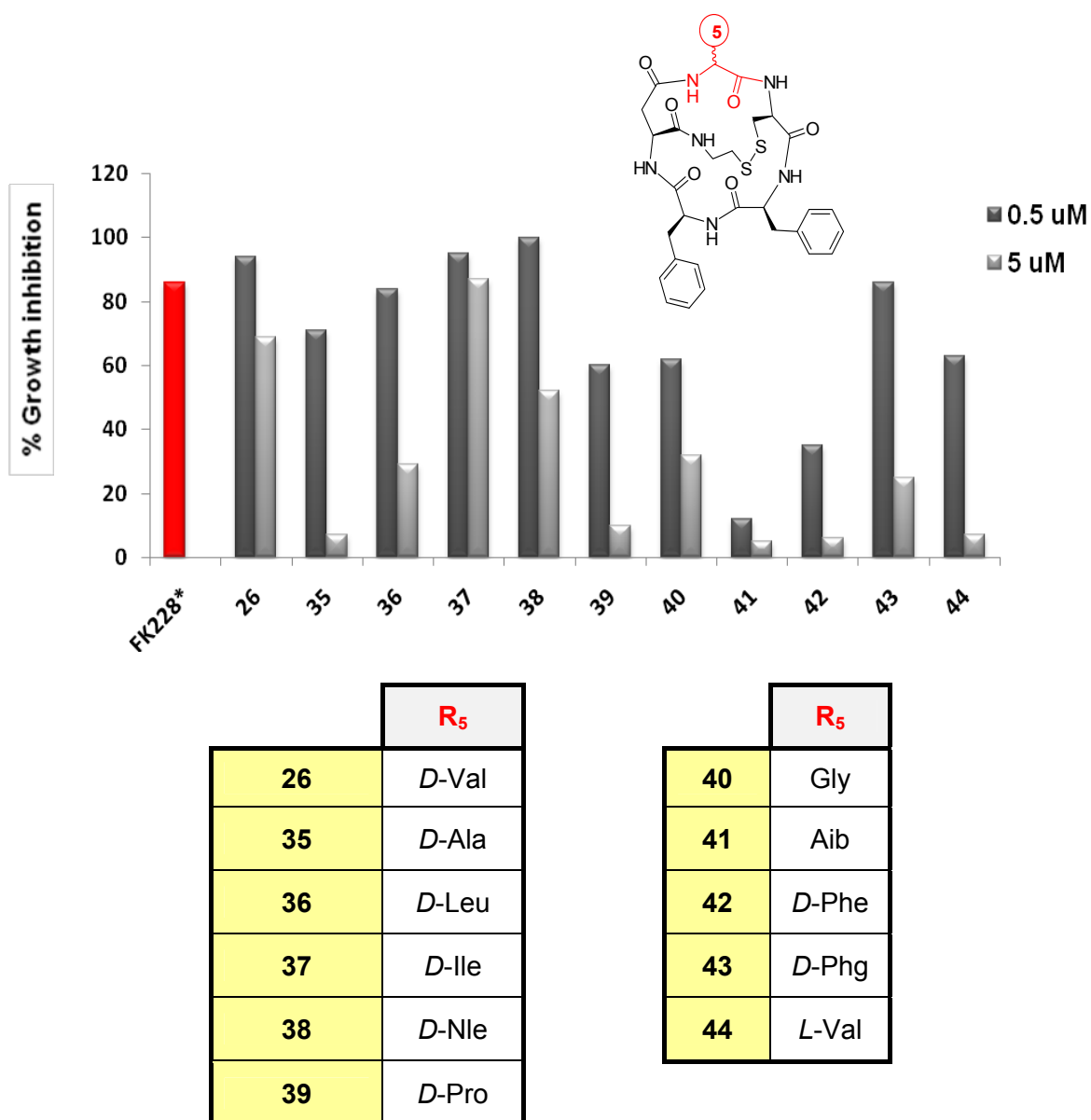
Figure 13. IV series of compounds

Also, a loss of potency was achieved introducing a further aromatic ring at the position 5 using amino acid like *D*-Phe and *D*-Phg, probably due to the excessive increment of the size of the molecules that impede the right interaction with the target (**42** and **43**). Finally, a significant difference of activity was observed for the compounds achieved with the introduction of amino-acids with aliphatic side chains. The presence of amino acid with no substitution or mono alkyl substituted on the β-carbon such as *D*-Ala, *D*-Leu and *D*-Nle resulted in compounds less potent of **26**. When the D-Val was replaced with a D-Ile an enhancement of activity was observed, leading to the compound **37**, which is about 3-fold more potent than **26**, suggesting that the β,β–dialkyl substitution of the *D*-amino-acid in position 5 helps to keep the right placement of the compound in its site of interaction.

4.3.5 Fifth series.

The fifth series of compounds was synthesized to investigate the requirements of the aromatic moieties at the position 2 and 3, replacing the two *L*-Phe of **26** with amino acids bearing aromatic ring with different distance from the backbone structure, size and electronic density.

First, the possibility to modify the distance of the aromatic moiety was evaluated introducing unnatural amino acids like *L*-Phg and L-Hph. As reported in the histogram in figure 6 the introduction of a single *L*-Phg at 3 lead to a slightly less potent compound (**45**). The replacement of the *L*-Phe at position 3 as well as the introduction of a *L*-Phg in both the positions resulted in completely inactivation (**46** and **47**).

Thus, the deletion of a β-carbon of both the *L*-Phe in **26** resulted in a loss of citoxicity which is more significant when the position 2 is replaced with a *L*-Phg (**46** and **47**). Successively, the distance between the aromatic rings at the positions 2 and 3 with the backbone structure was increased introducing a *L*-Hph. The replacement of the *L*-Phe at position 3 (**48**) produced a loss of potency, while the introduction of a *L*-Hph at position 2 provide the compound **49** which is slightly more potent than **26**. Interestingly when both the *L*-Phe were replaced with *L*-Hph, the resulted compound (**50**) showed higher antitumoral activity. Thus, while the loss of activity of the compound **48** along with what we have already observe for the compound **45** (*L*-Phg instead than *L*-Phe) seemed to exclude the possibility to vary the distance at the position 3, the enhancement of activity showed from the compound **49** indicated a better flexibility of the site of interaction of the aromatic ring in position **2** . Suddenly when two *L*-Hph were introduced (**50**) the negative effect of the replacement of the position 3 not only is compensated from

the presence of a second *L*-Hph at position 2, but even a kind of "synergistic" enhancement of activity was observed.

Next, the introduction of amino acids with increased size of the aromatic ring like *L*-2-Nal, *L*-1-Nal, *L*-Trp and *L*-Phe(4-Ph) was evaluated. As showed in the histogram in Figure 6, the replacement of the *L*-Phe at position 3 with *L*-2-Nal (**51**) leading a slightly increment of activity. The introduction of a *L*-2-Nal at position 2 provided the compound **52** which was less potent than **26.** According with the results achieved from the simultaneous replacement with two *L*-Hph, also the introduction of two *L*-2-Nal at the positions 2 and 3 of the compound **26**, produced a significant enhancement of activity leading to the most potent compound of this study (compound **53**, 100% inhibition at 0.5 μM, IC_{50} = 0.02 μM). The synthesis of three more compounds was performed using amino acids like *L*-1-Nal, *L*-Phe(4-Ph), *L*-Trp. First, the size of the aromatic ring was left invariated while its position was modified by using *L*-1-Nal instead than *L*-2-Nal (**54**). The activity of **54** (90% inhibition at 0.5 μM) was very similar to that showed from **53**, indicating that the modification of the placements of the two naphtyl groups is well tolerated from our structures. Next, the size of the aromatic rings was increased by replacing the two *L*-Phe with *L*-Phe(4-Ph) (**57**). The compound **57** showed citotoxicity at concentration similar to those previously observed for **26**, suggesting that this substitution is well tolerated but not productive in terms of activity.

The compound **55** was designed based on the information achieved from the studies on the modifications of the distance and the size of the aromatic rings, introducing a *L*-Hph at the position 3 and a *L*-2-Nal at the position 3. Unfortunately, no enhancement of activity was observed leading to the compound **55** which showed 80% inhibition at 0.5 μM.

The last modification on the size of the aromatic rings was performed replacing the two L-Phe of **26** with amino acids like L-Trp (**56**) that produced a completely loss of citotoxity probably due to the presence of the N^{In} that could represent a new potential point for the formation of hydrogen bonds that impedes the compound to reach the site of interaction.

Finally, the introduction of aromatic amino acids para-substituted with electron donators and acceptors groups as L-Phe(4-F), L-Phe(4-NO$_2$) was evaluated in order to see if the strength of the interaction of the aromatic rings could be increased. The compounds **58** and **59** resulting from the introduction of a L-Phe(4-F) respectively at the positions 2 and 3 did not show any significant enhancement of activity if compared with **26**..

Conversely, the introduction of L-Phe(4-NO$_2$) at the position 2 and 3 (compounds **60** and **61**) produced compounds slightly less potent then **26.** Thus, the effects of the electron donators or acceptors on the activity was not fundamental and the loss of activity observed with **60** and **61** is probably due to the increment of polarity.

Last, we designed the hybrid compound **62** which was synthesized combining the structural features of the two most active analogues reported in the fourth and fifth series (**37** and **53**) in order to produce a "synergistic" enhancement of potency. The compound **62** was constructed keeping two L-Nal at the positions 2 and 3 while the D-Val at position 5 was replaced with D-Ile. Unfortunately, the desired enhancement of citotoxicity was not observed, and a compound less potent than **53** was achieved, probably due to the excessive increment of the size of the structure that loses the capability to correctly interact with the target inside the cells.
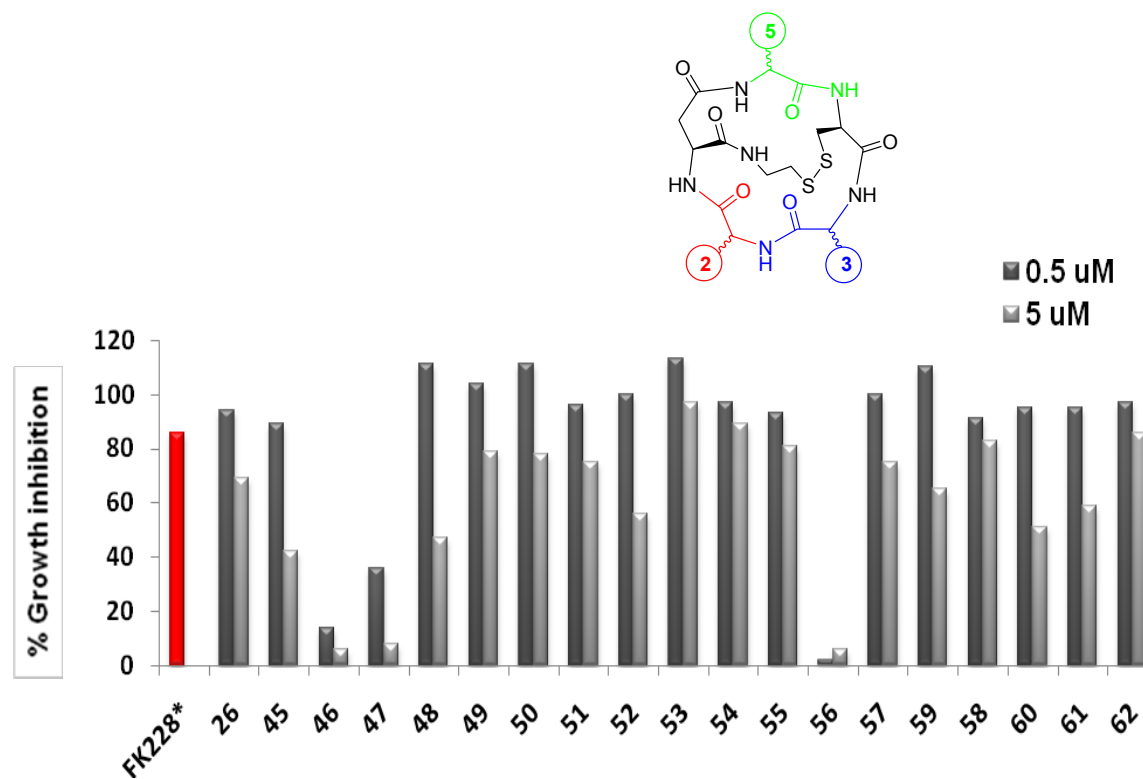
	R₂	R₃	R₅		R₂	R₃	R₅
26	*L*-Phe	*L*-Phe	*D*-Val	**54**	*L*-Nal(1')	*L*-Nal(1')	*D*-Val
45	*L*-Phe	*L*-Phg	*D*-Val	**55**	*L*-Hph	*L*-Nal(2')	*D*-Val
46	*L*-Phg	*L*-Phe	*D*-Val	**56**	*L*-Trp	*L*-Trp	*D*-Val
47	*L*-Phg	*L*-Phg	*D*-Val	**57**	*L*-Phe(4-Ph)	*L*-Phe(4-Ph)	*D*-Val
48	*L*-Phe	*L*-Hph	*D*-Val	**58**	*L*-Phe	*L*-Phe(4-F)	*D*-Val
49	*L*-Hph	*L*-Phe	*D*-Val	**59**	*L*-Phe(4-F)	*L*-Phe	*D*-Val
50	*L*-Hph	*L*-Hph	*D*-Val	**60**	*L*-Phe	*L*-Phe(4-NO₂)	*D*-Val
51	*L*-Phe	*L*-Nal(2')	*D*-Val	**61**	*L*-Phe(4-NO₂)	*L*-Phe	*D*-Val
52	*L*-Nal(2')	*L*-Phe	*D*-Val	**62**	*L*-Nal(2')	*L*-Nal(2')	*D*-Ile
53	*L*-Nal(2')	*L*-Nal(2')	*D*-Val				

Figure 14. V series of compounds

4.4 Structure-Activity Relationship (summary)

As summarized below, the results of MTT-assay provided enough information to accomplish exhaustive Structure-activity relationship study that clarified the structural requirements of each position required for the antitumoral activity (Figure 15).
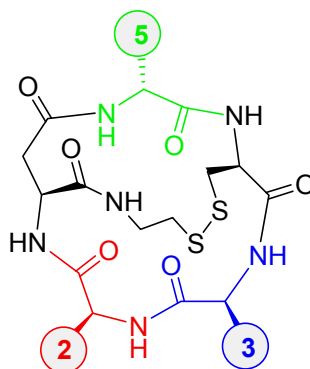
R_2	R_3	R_5
L-C$^{\alpha}$	L-C$^{\alpha}$	D-C$^{\alpha}$
Aromatic > Aliphatic > Polar	Aromatic > Aliphatic > Polar	Aliphatic > Aromatic > Polar
Nal(2') > Nal(1') > Hph > Phe	Nal(2') > Nal(1') > Hph > Phe	D-Val and D-Ile > D-Nle > D-Leu > D-Ala
Polar and aliphatic amino acids are not tolerated	Polar amino acids are not tolerated	Polar amino acids are not tolerated

Figure 15. Structure-Activity relationship

Position 2. The presence of *L*-aromatic side chain amino acids is necessary for the antitumoral activity. The increment of the size of the aromatic rings such as Naphtyl instead than Phenyl group is preferred to achieve enhancement of activity. The introduction of aliphatic or polar side chains amino acids is not well tolerated.

Position 3. *L*-aromatic side chain amino acids are necessary for the antitumoral activity. The increment of the size of the aromatic rings such as Naphtyl instead than Phenyl group is preferred to achieve enhancement of activity. The introduction of aliphatic or polar side chains amino acids is not well tolerated.

Position 5. *D*-aliphatic side chain amino acids are necessary for the antitumoral activity. The presence of a β,β-disubstituted carbon such as D-Val and D-Ile is required to achieve enhancement of activity. The introduction of aliphatic or polar side chains amino acids is not well tolerated.

4.5 Antitumor activity (II part)

The last part of the MTT study was conceived to confirm the effective capability of our analogues as antitumor agents. Two representative compounds were selected (**26** and **53**) and tested on a panel of six different cancer cell lines (prostate and bladder) at concentrations of 0.001, 0.01, 0.1, 0.5, 1 and 5 μM (Figure 16). Both the compounds showed to strongly inhibit the growth of all six cancer cell lines. Comparison between the activities evidenced that the compound **53** confirmed to be more potent than **26** on each single cancer cell line, showing growth inhibition at nanomolar concentrations comparable with those reported for FK228.
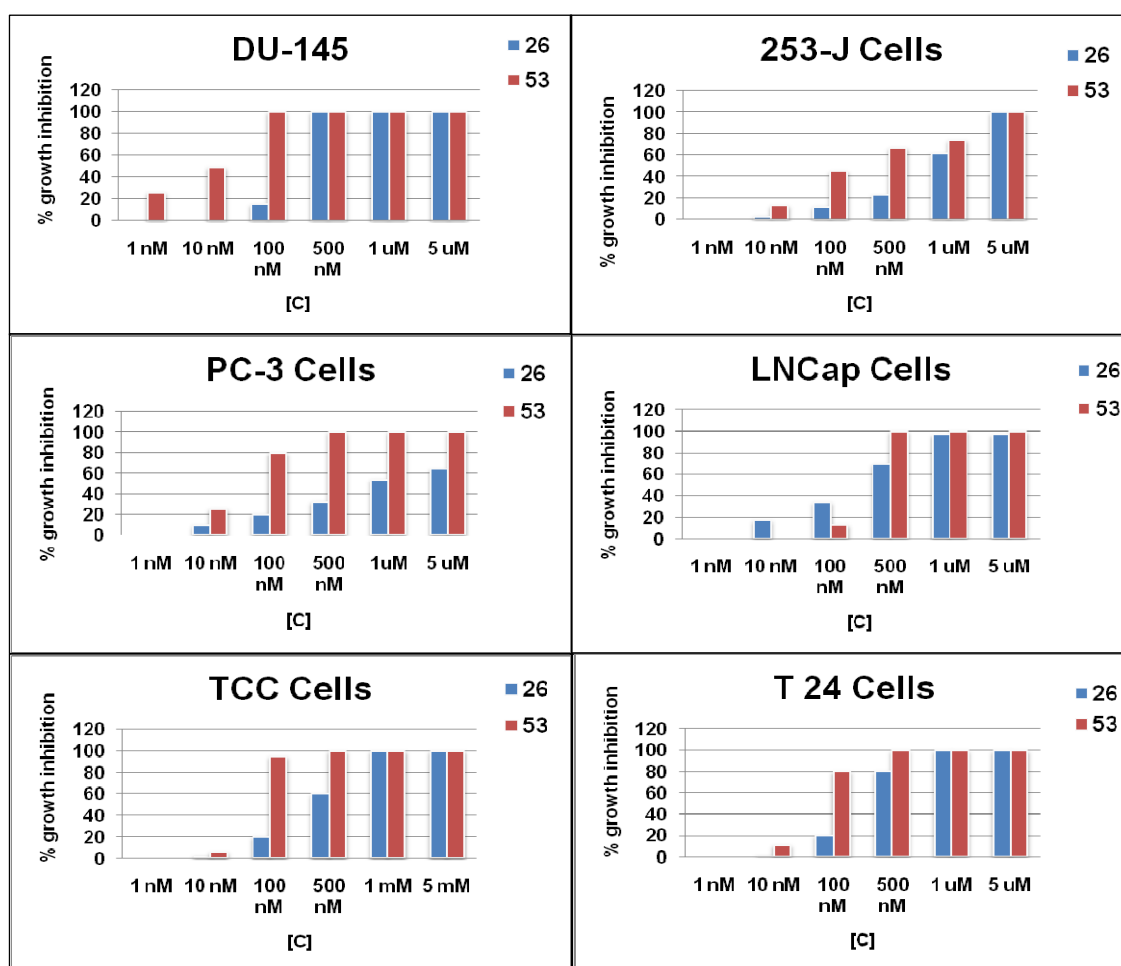
Figure 16. Antitumoral activity of 26 and 53 on various cancer cells.

4.5 HDAC assay.

To evaluate that the antitumor activity of our analogues resulted from the same mechanism of action previously described for FK228, the compounds **26** and **53**, which have been previously selected for the MTT assay on six cancer cell lines, were tested as HDAC inhibitors using cell nuclear extract of urinary bladder cancer cells T24.

FK228 has been reported to behave as prodrug that becomes activated through the reduction of the disulphide bridge releasing the sulfidrilic function of the (*3S,4E*)-3-hydroxy-7-mercapto-4-heptenoic acid that interacts with a Zn^{++} atom placed on the bottom of the active site of the HDACs. To investigate the effective capability of FK228 to inhibit isolated HDAC enzymatic isoforms, Furumai *et al.* tested it as reduced form preincubating FK228 with a solution of a reductive agent like DTT at a concentration that did not invalidate the results of the test.[102] Thus, for our analogues we replied the same test condition reducing them by the treatment with an ethanolic solution of DTT 100 μM.

The reduction of the disulphide bridge was monitored by analytical HPLC and stopped at 12 h when no significant amount of the oxidized form could be detected.
As reported in Figure 7, both the compounds tested did not show significant capability to inhibit the HDACs activity at the same concentrations that were observed to effect the tumor cell growth.

Thus, our hypothesis of modification resulted in structural modifications of the original FK228 that inactivate its original HDAC-related mechanism of action. However, as mentioned in the MTT assay results, at least one of our analogues (**53**) has kept the antitumor activity at concentration comparable to those exhibited from FK228.
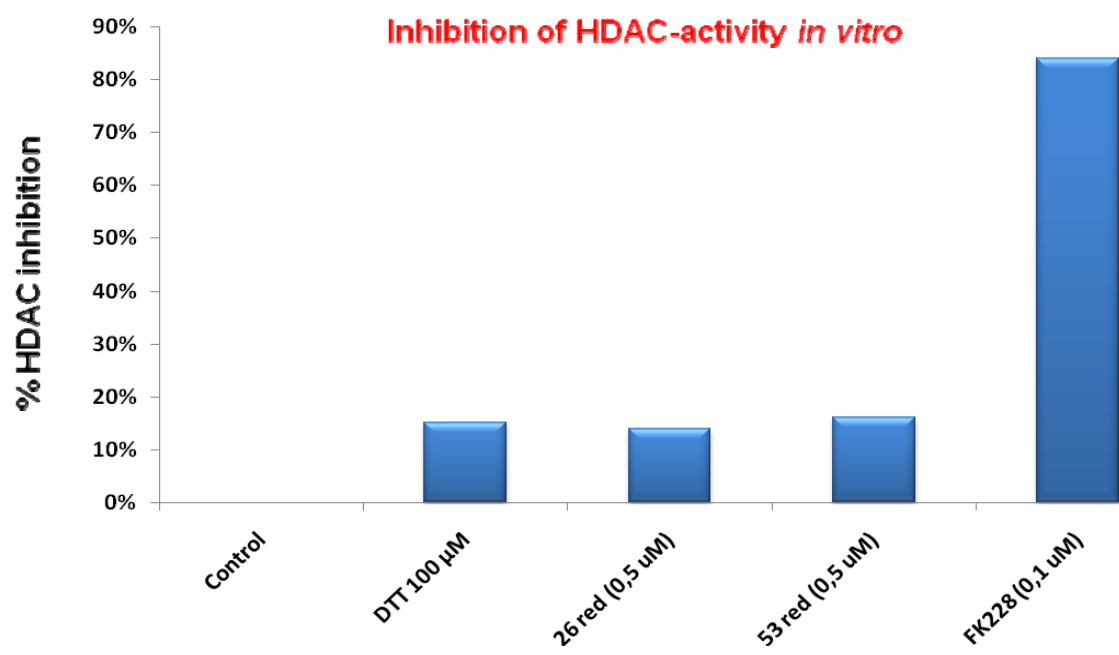
Figure 16. HDAC activity of 26 and 53

5. CONCLUSION

In summary, we have designed a novel FK228 analogue by simple isosteric replacement, and the modifications enabled rapid and efficient synthesis of a number of FK228 analogues in solid-phase.

Structure-activity study of a total of 62 FK228 analogues have revealed a new compound (**53**) with high antitumoral activity on various cancer cells. Moreover, HDAC-inhibition and the MTT studies clearly evidenced an unexpected loss of correlation between the antitumor activity and HDACs inhibition, that needs to be further investigated.

Based on the preliminary information in our hands we have formulated two hypothesis to explain the unexpected trend of our compounds.

1. The introduction of the aspartilcysteamine moiety into the original FK228 produces noteworthy structural changes that result in a loss of the characteristics required to inhibit HDACs, which is compensated from the acquisition of a new capability to interact with an alternative target.

2. Our analogues partially mimic the activity of FK228, that could normally interact with an additional target apart from HDACs inside the cells which have been not yet highlighted.

In any instances, it is our opinion that this study represent an exceptional starting point that could be accomplished following two alternative directions.

First, an in-depth biological study is required to provide the answers to the unsolved questions emerged in the course of the study, resulting in the identification of a new potential target for intervention in oncology.

Finally, alternative isosteric modifications of the (*3S,4E*)-3-hydroxy-7-mercapto-4-heptenoic acid should be hypothesized using similar building blocks, in order to restore the original HDACs-related activity keeping the synthetic advantages highlighted in this study.

6. EXPERIMENTAL SECTION

6.1 Materials

N^α-Fmoc-protected amino acids, 5-(4-formyl-3,5-dimethoxyphenoxy)butyric acid (BAL), aminomethyl-polystyrene (AM-PS) resin and bromo-tris-pyrrolidino phosphoniumhexafluorophosphate (PyBrOP) were purchased from EMD Biosciences (San Diego, CA). O-Benzotriazole-N,N,N',N'-tetramethyl-uronium-hexafluoro-phosphate (HBTU), N-hydroxybenzotriazole (HOBt), benzotriazolyloxytris-(dimethylamino)phosphonium hexafluorophosphate (BOP) and tetramethylfluoro-formamidinium hexafluorophosphate (TFFH) were purchased from Advanced ChemTech (Louisville, KY). Disopropyl carbodiimide (DIC), N,N-diisopropylethylamine (DIEA), sodium cyanoborohydride, pyridine and trityl chloride were purchased from Acros Organics (Morris Plains, NJ). Tosyl chloride was purchased from Alfa Aesar (Ward Hill, MA). Triisopropylsilane (TIS), cysteamine hydrochloride, 5,5'-dithiobis(2-nitrobenzoic acid) (Ellmann's reagent) and 1,8-Diazabicyclo[5.4.0]-undec-7-ene (DBU) were purchased from Sigma-Aldrich (St. Louis, MO). N^α-Fmoc-protected amino acids, the following side chain protecting groups were used: Asp(OAl), Cys(Trt), Thr(tBu) and Trp(N^{in}-Boc). Solvents and reagents were reagent grade and used without further purification unless otherwise noted.

Analytical thin-layer chromatography was performed on silica gel plates (250 μm; Sorbent Technologies, Atlanta, GA). Column chromatography was carried out using flash-grade silica gel (mesh 230-400; Sorbent Technologies, Atlanta, GA). ^{1}H and ^{13}C-NMR spectra were acquired on JEOL ECLIPSE 270 (270 MHz) NMR spectrometer. All synthesized compounds were analyzed by analytical HPLC (Agilent 1100 series HPLC

system) equipped with a C_{18}-bounded analytical reverse-phase HPLC column (Vydac 218TP104, 4.6 x 250 mm) using a gradient elution (10 to 90% acetonitrile in water (0.1% TFA) over 40 min; flow rate = 1.0 mL/min; diode-array UV detector). Accurate molecular weights of compounds were confirmed by ESI-mass spectrometry using an Applied Biosystem 4000 Q TRAP® LC/MS/MS System.

6.2 *S2*-(Trityl)cysteamine hydrochloride

Cysteamine hydrochloride (200 mg, 1.73 mmol) was dissolved in DCM-DMF (1:1, 10 mL). Trityl chloride (725 mg, 2.60 mmol) was added to the solution, and the reaction mixture was stirred for 2 h at room temperature. Then, the solution was concentrated in vacuo and subsequently co-concentrated with toluene (3 ×15 mL), ethanol (3 ×15 mL), and dichloromethane (3 ×15 mL). The product was purified by column chromatography (DCM/MeOH, 9:1) to yield pure compound (500 mg, 90% yield). R_f 0.63 (DCM/MeOH, 9:1). ^{1}H NMR (270 MHz, CDCl$_3$): δ = 2.26 (t, 2H), 2.60 (t, 2 H), 7.15-7.29 (m, 9H) and 7.40-743 (m, 6 H). ^{13}C NMR (270 MHz, CD$_3$OD): δ = 38.42, 67.07, 126.83, 127.84, 129.36, 144.36.
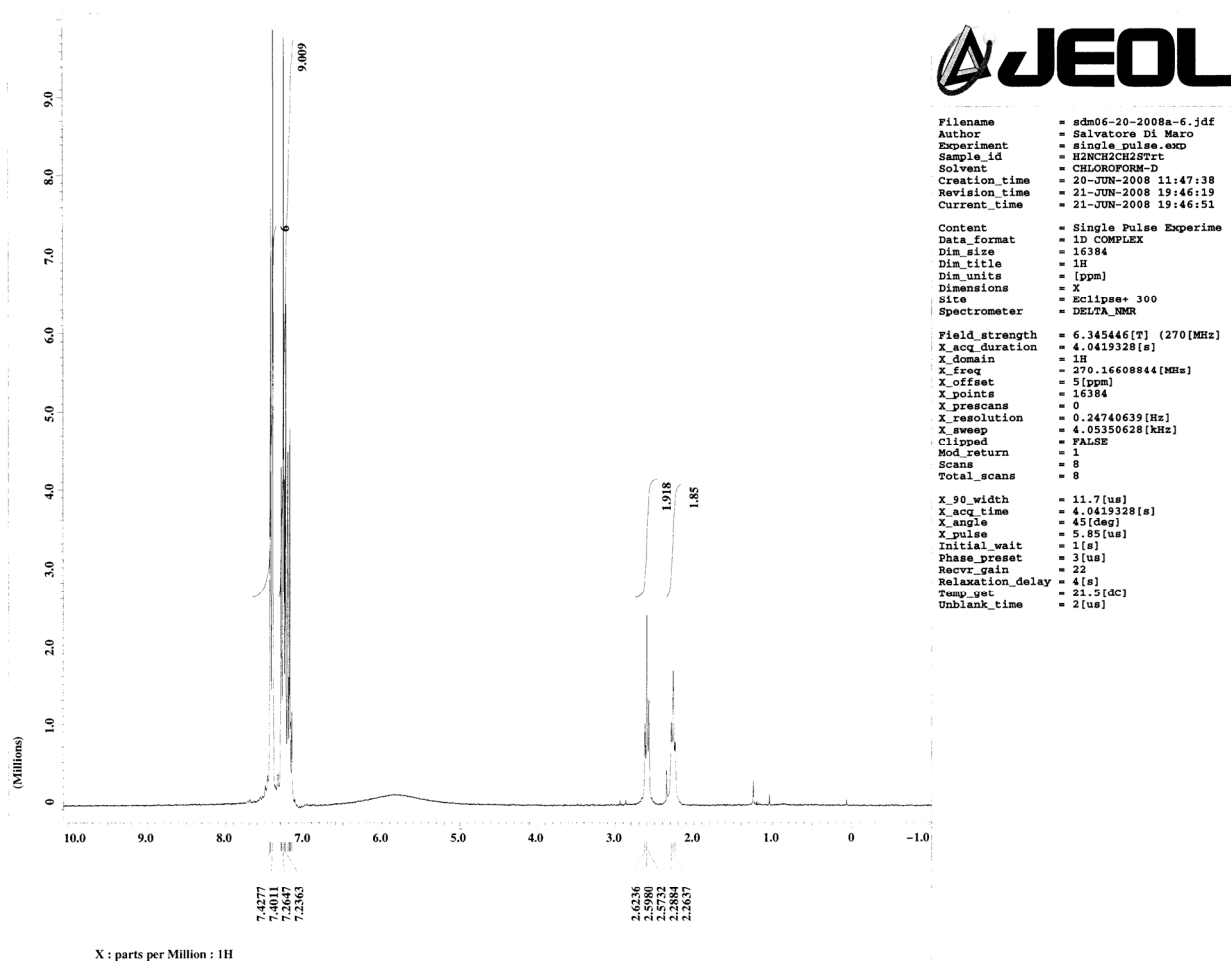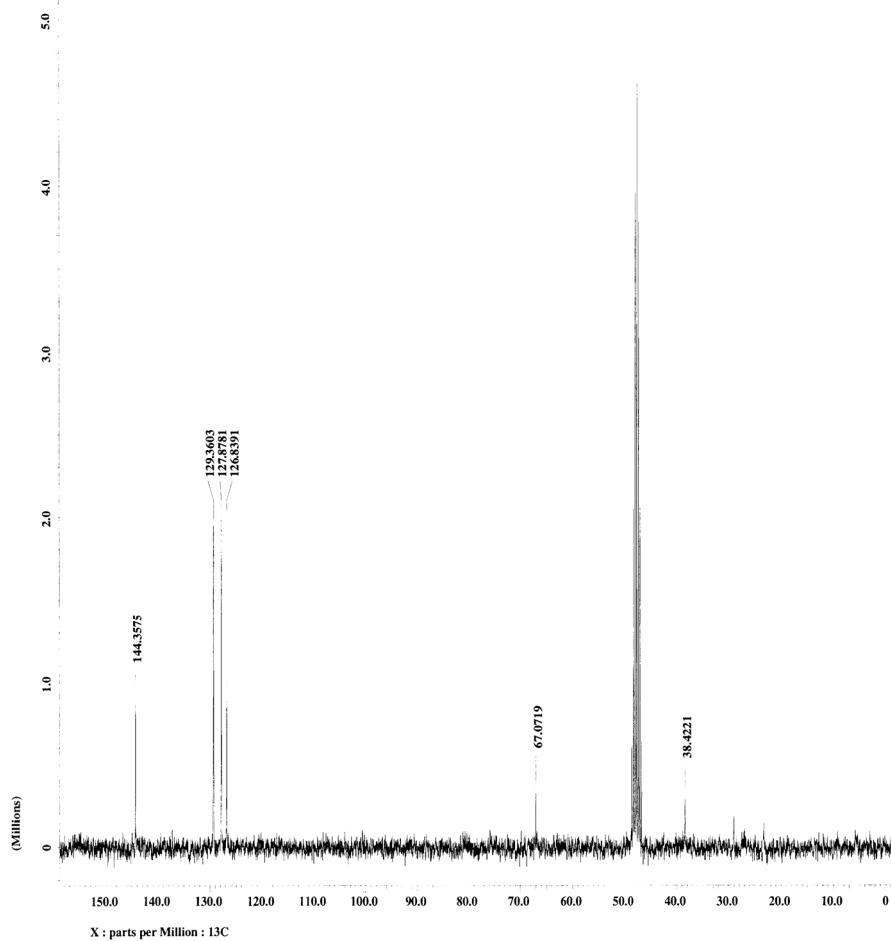
Filename   = sdm06-20-2008a-6.jdf
Author   = Salvatore Di Maro
Experiment   = single_pulse.exp
Sample_id   = H2NCH2CH2STrt
Solvent   = CHLOROFORM-D
Creation_time   = 20-JUN-2008 11:47:38
Revision_time   = 21-JUN-2008 19:46:19
Current_time   = 21-JUN-2008 19:46:51

Content   = Single Pulse Experime
Data_format   = 1D COMPLEX
Dim_size   = 16384
Dim_title   = 1H
Dim_units   = [ppm]
Dimensions   = X
Site   = Eclipse+ 300
Spectrometer   = DELTA_NMR

Field_strength = 6.345446[T] (270[MHz]
X_acq_duration = 4.0419328[s]
X_domain   = 1H
X_freq   = 270.16608844[MHz]
X_offset   = 5[ppm]
X_points   = 16384
X_prescans   = 0
X_resolution   = 0.24740639[Hz]
X_sweep   = 4.05350628[kHz]
Clipped   = FALSE
Mod_return   = 1
Scans   = 8
Total_scans   = 8

X_90_width   = 11.7[us]
X_acq_time   = 4.0419328[s]
X_angle   = 45[deg]
X_pulse   = 5.85[us]
Initial_wait   = 1[s]
Phase_preset   = 3[us]
Recvr_gain   = 22
Relaxation_delay = 4[s]
Temp_get   = 21.5[dc]
Unblank_time   = 2[us]

X : parts per Million : 1H

X : parts per Million : 13C

6.3 General method for Peptide Synthesis (61-69)

250 mg AM-PS resin (0.46 mmol/g, 0.115 mmol) was swelled in DMF over 1 h, and a DMF solution (2 mL) of 4-(4-formyl-3,5-dimethoxyphenoxy)butyric acid (46.3 mg, 1.5 equiv), HBTU (65.4 mg, 1.5 equiv), HOBt (26.4 mg, 1.5 equiv), DIEA (60 μL, 3.0 equiv) was added to the resin. The mixture was shaken for 12 h, and after washed the resin with DMF (3 × 1 min) the Kaiser ninhydrin and TNBS tests[115-116]of the resin were found negative. Then, reductive amination was performed using S-tritylcysteamine hydrochloride (163.7 mg, 4 equiv) and NaBH$_3$CN (28.9 mg, 4 equiv) in DMF (4 mL) at room temperature for 12 h. After the reaction was finished, the resin was washed with DMF (3 × 1 min) and showed positive result by p-chloroanilin test,[117] indicating the formation of the secondary amine (**63**).

The coupling of the first amino acid was carried out using Fmoc-Asp(OAl) (181.9 mg, 4 equiv), DIC (36 μL, 2 equiv), and DIEA (40 μL, 2 equiv) with DMF/DCM (1:1) for 12 h (**63**). After the resin was washed with DMF (3 × 1 min) and a negative p-chloranilin test was observed. The yield of the coupling reaction using the symmetric anhydride was determined by measuring the level of the amino acid attachment as described below. To dried resin (10 mg), was added DBU/DMF (2% v/v, 2 mL) and the resulting mixture was gently shaken for 30 min. Then, the solution was diluted to 10 mL with CH$_3$CN. Aliquot of the solution (2 mL) was further diluted to 25 mL with CH$_3$CN for measuring UV absorbance. On the other hand, a reference solution was prepared without the resin. UV adsorbance of the solution at 304 nm was measured using a UV/Vis spectrophotometer (Agilent Technology, 89090A), and the Fmoc loading level was calculated by the following equation.

Fmoc loading (mmol/g) = (Abs$_{sample}$ – Abs$_{ref}$) x 16.4/mg of resin.

As summarized in Table 1, the coupling reaction with the symmetric anhydride of Fmoc-Asp(OAl) was found to be most effective (98% yield) compared to other reagents used.

Next, the N^α-Fmoc protecting group of Asp(OAl) was removed by the treatment with piperidine (20% in DMF; 1×5 min and 1×25 min). The resin was washed with DMF (3×1 min) and the coupling of the second amino acid was performed using Fmoc-AA$_1$ (4 equiv) with HBTU (174.6 mg, 4 equiv), HOBt (70.5 mg, 4 equiv) and DIEA (160 µL, 8 equiv) in DMF (4 mL) for 2 h at room temperature (**64**). After 2 h the resin was washed with DMF (3×1 min), the Kaiser ninhydrin test of the resin was found negative. The coupling of the remaining amino acids (Fmoc-AA$_2$, Fmoc-D-Cys(Trt), and Fmoc-AA$_3$) was performed repeating the steps described above. The synthesis of the linear peptides (**67**) was monitored by analytical HPLC which showed one major peak (> 95% purity) that was later confirmed by HR-ESI-MS.

After the construction of the linear peptides (**67**), the allyl protecting group of Asp was removed by treating the resin with tetrakis(triphenyphosphine)-palladium(0) (13.3 mg, 0.1 equiv) and N,N'-dimethylbarbituric acid (179.4 mg, 10 equiv) in DCM/DMF (3:1, 3 mL) for 30 min at room temperature under nitrogen atmosphere, and the reaction was repeated again. After the resin was washed with DMF (3×1 min), the Fmoc group of D-Val was removed with piperidine (20% in DMF; 1×5 min, 1×30 min) and the resin was washed with DCM (3×1 min) and DMF (3×1 min). The lactam bond was formed by the treatment with HBTU (261.7 mg, 6 equiv), HOBt (105.7 mg, 6 equiv), and DIEA (240 µL, 12 equiv) in DMF (3 mL) for 3 h (**68**). When the reaction was finished, the resin washed with DMF (3×1 min), the formation of the monocyclic compound (4a-l) was monitored by Kaiser ninhydrin test and analytical HPLC after cleaving small

amount of resin (about 10 mg). No detectable amount of the linear peptides was left indicating high yield in cyclization (> 95%).

The S-Trt protecting groups were removed by dilute TFA (1% in DCM, 5 × 2 min) and the release of free thiol was monitored by Ellmann's test.[118] Then the resin was washed with DCM (3 × 1 min) and DMF (3 × 1 min), and the oxidation of thiols was carried out by using I_2 (292 mg, 10 equiv) and DIEA (100 µL, 5 equiv) in DCM (4 mL) for 30 min at room temperature (**69**). After the reaction was finished, no significant amount of the monocyclic peptide was detected by analytical HPLC. Then, the resin was washed with DMF (3 × 1 min) and DCM (3 × 1 min) and dried in vacuo overnight.

The bicyclic FK228 analogues (5a-l) was cleaved from the resin by the treatment with TFA/TIS/water (10 mL, 90:5:5) for 3 h at room temperature. Then, the resin was filtered and the TFA solution was concentrated under gentle stream of nitrogen to the volume of approximately 1 mL. The peptide was precipitated by adding cold diethyl ether (20 mL) and centrifuged. The washing with diethyl ether was repeated again and the resulting product was dried overnight, followed by characterization by analytical HPLC and high-resolution ESI-MS.

6.3.1 Compound 69

The monocyclic compound (**70**) containing Thr at the position of Z-Dhb was prepared by following the same procedures described above. To create Z-Dhb on resin, the β-hydroxy group of Thr was tosylated by treating the resin with tosyl chloride (110 mg, 5 equiv) in pyridine (186 μL, 20 equiv). The reaction was carried out for 30 min at room temperature, and monitored by analytical HPLC by cleaving small amount of the resin. No significant amount of starting material with the free hydroxyl group was observed. Then, the resin was washed with DMF (3 x 1 min) and DCM (3 x 1 min) and the tosylated peptide was treated with DBU (172 μL, 10 equiv) in DMF (3 ml) for 24 h to produce a monocyclic peptide containing Z-Dhb (**70**). After washing the resin with DMF (3 × 1 min), the reaction was monitored by analytical HPLC and one major peak (> 90%) was observed.

Compounds 1 and 34 (Oxydation with I$_2$). The S-Trt protecting groups of the intermediate **70** were removed by dilute TFA (1% in DCM, 5 × 2 min) and the release of free thiol was monitored by Elmann's test.[26] Then the resin was washed with DCM (3 × 1 min) and DMF (3 × 1 min) and the oxidation of thiols was carried out by using I$_2$ (292 mg, 10 equiv) and DIEA (100 μL, 5 equiv) in DCM (4 mL) for 30 min at room temperature. After the reaction was finished, the resin was washed wit DMF (5 × 1 min) and no significant amount of the monocyclic peptide was detected by analytical HPLC. Then, the resin was washed with DMF (3 × 1 min) and DCM (3 × 1 min) and dried in vacuo overnight.

The bicyclic FK228 analogues (**1 and 34**) was cleaved from the resin by the treatment with TFA/TIS/water (10 mL, 90:5:5) for 3 h at room temperature. Then, the resin was filtered and the TFA solution was concentrated under gentle stream of nitrogen to the

volume of approximately 1 mL. The peptide was precipitated by adding cold diethyl ether (20 mL) and centrifuged. The washing with diethyl ether was repeated again and the resulting product was dried overnight, followed by characterization by analytical HPLC and high-resolution ESI-MS.

Compounds 1 and 34 (Oxydation with DMSO)*.* The monocyclic intermediate **70** was cleaved from the resin by the treatment with TFA/TIS/water (10 mL, 90:5:5) for 3 h at room temperature. Then, the resin was filtered and the TFA solution was concentrated under gentle stream of nitrogen to the volume of approximately 1 mL. The peptide **71** was precipitated by adding cold diethyl ether (20 mL) and centrifuged. The washing with diethyl ether was repeated again and the resulting product was dried overnight. The peptide **71** was recovered and solubilized in a solution of CH_3OH/H_2O (9:1 100 ml) and $NaHCO_3$ (38 mg, 4 eq) and DMSO (2ml) were added. The solution was stirred for 36 h, when not detectable amount of monocyclic compound could be observed by analytical HPLC. Next, the CH_3OH was evaporated and 50 ml of EtOAc were added. The organic layer was extracted with 1 N HCl (3 x 25 ml), satured $NaHCO_3$ (3 x 25 ml), H_2O (3 x 25 ml) and satured NaCl (3 x 25 ml) and dried with anhydrous Na_2SO_4. Finally, the EtOAc was evaporated and the final product was dried overnight, followed by characterization by analytical HPLC and high-resolution ESI-MS.

6.4 Biological assay to determine antitumor activity

Human transitional carcinoma cell lines T24, TCCSUP, 253J and human prostate cancer cell lines PC-3, LNCaP, Du-145 were cultured in T medium (Invitrogen) supplemented with 5% fetal bovine serum and 1% penicillin-streptomycin. $2x10^3$ Cells in 50 µL of medium were plated into each well of a 96-well plate one day before adding compound. Each compound was diluted with DMSO to two folds of the concentrations, then 50 µL of the compound-containing medium was added into cells. Each treatment was performed in triplicate on the same plate. For each compounds reported the treatments were repeated at least three times on different plates. Three days later, cell proliferation was measured with a cell proliferation kit (Roche). Briefly, 10 µL of MTT (3-[4,5-dimethylthiazol-2yl]-2,5-diphenyl tetrazolium bromide) was added into each well for 4 h, then 100 µL of the solubilization solution was added and cells were incubated for overnight. The spectrophotometrical absorbance of the samples was measured with a SpectraMax M5 plate reader (Molecular Devices) at 565 nm. The data were presented as percentage inhibition using non-treated cells as control.

7. Table of characterization

1: 48.0 mg, overall yield: 75%, purity: 85%, t_R 14.6 min (analytical HPLC, 10 to 90% acetonitrile in water (0.1% TFA) over 40 min, flow rate of 1.0 mL/min), molecular formula: $C_{23}H_{36}N_6O_6S_2$, calculated mass: 556.2138, found: 556.2126.

2: 50.7 mg, overall yield: 81%, purity: 94%, t_R 13.1 min (analytical HPLC, 10 to 90% acetonitrile in water (0.1% TFA) over 40 min, flow rate of 1.0 mL/min), molecular formula: $C_{22}H_{36}N_6O_6S_2$, calculated mass: 544.2138, found: 544.2154.

3: 50.0 mg, overall yield: 75%, purity: 90%, t_R 16.6 min (analytical HPLC, 10 to 90% acetonitrile in water (0.1% TFA) over 40 min, flow rate of 1.0 mL/min), molecular formula: $C_{24}H_{40}N_6O_6S_2$, calculated mass: 572.2451, found: 572.2450.

4: 51.0 mg, overall yield: 76%, purity: 82%, t_R 16.7 min (analytical HPLC, 10 to 90% acetonitrile in water (0.1% TFA) over 40 min, flow rate of 1.0 mL/min), molecular formula: $C_{25}H_{42}N_6O_6S_2$, calculated mass: 586.2607, found: 586.2626.

5: 54.0 mg, overall yield: 80%, purity: 81%, t_R 16.8 min (analytical HPLC, 10 to 90% acetonitrile in water (0.1% TFA) over 40 min, flow rate of 1.0 mL/min), molecular formula: $C_{25}H_{42}N_6O_6S_2$, calculated mass: 586.2607, found: 586.2626.

6: 49.2 mg, overall yield: 75%, purity: 80%, t_R 17.0 min (analytical HPLC, 10 to 90% acetonitrile in water (0.1% TFA) over 40 min, flow rate of 1.0 mL/min), molecular formula: $C_{24}H_{38}N_6O_6S_2$, calculated mass: 570.2294, found: 570.2267.

7: 47.6 mg, overall yield: 78%, purity: 81%, t_R 12.9 min (analytical HPLC, 10 to 90% acetonitrile in water (0.1% TFA) over 40 min, flow rate of 1.0 mL/min), molecular formula: $C_{21}H_{34}N_6O_6S_2$, calculated mass: 530.1981, found: 530.1955.

8: 60.3 mg, overall yield: 85%, purity: 87%, t_R 19.6 min (analytical HPLC, 10 to 90% acetonitrile in water (0.1% TFA) over 40 min, flow rate of 1.0 mL/min), molecular formula: $C_{28}H_{40}N_6O_6S_2$, calculated mass: 620.2451, found: 620.2462.

9: 66.7 mg, overall yield: 88%, purity: 92%, t_R 23.1 min (analytical HPLC, 10 to 90% acetonitrile in water (0.1% TFA) over 40 min, flow rate of 1.0 mL/min), molecular formula: $C_{30}H_{41}N_7O_6S_2$, calculated mass: 659.2560, found: 659.2581.

10: 62.2 mg, overall yield: 90%, purity: 87%, t_R 11.1 min (analytical HPLC, 10 to 90% acetonitrile in water (0.1% TFA) over 40 min, flow rate of 1.0 mL/min), molecular formula: $C_{25}H_{43}N_7O_6S_2$, calculated mass: 601.2716, found: 601.2724.

11: 61.0 mg, overall yield: 87%, purity: 84%, t_R 12.3 min (analytical HPLC, 10 to 90% acetonitrile in water (0.1% TFA) over 40 min, flow rate of 1.0 mL/min), molecular formula: $C_{25}H_{38}N_8O_6S_2$, calculated mass: 610.2356, found: 610.2388.

12: 59.5 mg, overall yield: 88%, purity: 80%, t_R 13.3 min (analytical HPLC, 10 to 90% acetonitrile in water (0.1% TFA) over 40 min, flow rate of 1.0 mL/min), molecular formula: $C_{23}H_{36}N_6O_8S_2$, calculated mass: 588.2036, found: 588.2075.

13: 56.1 mg, overall yield: 85%, purity: 85%, t_R 13.6 min (analytical HPLC, 10 to 90% acetonitrile in water (0.1% TFA) over 40 min, flow rate of 1.0 mL/min), molecular formula: $C_{23}H_{38}N_6O_7S_2$, calculated mass: 574.2243, found: 574.2242.

14: 52.6 mg, overall yield: 78%, purity: 84%, t_R 19.2 min (analytical HPLC, 10 to 90% acetonitrile in water (0.1% TFA) over 40 min, flow rate of 1.0 mL/min), molecular formula: $C_{25}H_{42}N_6O_6S_2$, calculated mass: 586.2607, found: 586.2630.

15: 51.3 mg, overall yield: 82%, purity: 79%, t_R 13.5 min (analytical HPLC, 10 to 90% acetonitrile in water (0.1% TFA) over 40 min, flow rate of 1.0 mL/min), molecular formula: $C_{22}H_{36}N_6O_6S_2$, calculated mass: 544.2138, found: 544.2159.

16: 51.4 mg, overall yield: 80%, purity: 83%, t_R 14.9 min (analytical HPLC, 10 to 90% acetonitrile in water (0.1% TFA) over 40 min, flow rate of 1.0 mL/min), molecular formula: $C_{23}H_{38}N_6O_7S_2$, calculated mass: 558.2294, found: 558.2324.

17: 53.9 mg, overall yield: 84%, purity: 78%, t_R 15.2 min (analytical HPLC, 10 to 90% acetonitrile in water (0.1% TFA) over 40 min, flow rate of 1.0 mL/min), molecular formula: $C_{23}H_{38}N_6O_6S_2$, calculated mass: 558.2294, found: 558.2312.

18: 57.2 mg, overall yield: 84%, purity: 82%, t_R 16.6 min (analytical HPLC, 10 to 90% acetonitrile in water (0.1% TFA) over 40 min, flow rate of 1.0 mL/min), molecular formula: $C_{26}H_{36}N_6O_6S_2$, calculated mass: 592.2138, found: 592.2118.

19: 58.0 mg, overall yield: 88%, purity: 86%, t_R 10.8 min (analytical HPLC, 10 to 90% acetonitrile in water (0.1% TFA) over 40 min, flow rate of 1.0 mL/min), molecular formula: $C_{23}H_{39}N_7O_6S_2$, calculated mass: 573.2403, found: 573.2418.

20: 50.1 mg, overall yield: 78%, purity: 81%, t_R 15.7 min (analytical HPLC, 10 to 90% acetonitrile in water (0.1% TFA) over 40 min, flow rate of 1.0 mL/min), molecular formula: $C_{23}H_{38}N_6O_6S_2$, calculated mass: 558.2294, found: 558.2315.

21: 54.8 mg, overall yield: 85%, purity: 75%, t_R 12.2 min (analytical HPLC, 10 to 90% acetonitrile in water (0.1% TFA) over 40 min, flow rate of 1.0 mL/min), molecular formula: $C_{21}H_{32}N_6O_8S_2$, calculated mass: 560.1723, found: 560.1745.

22: 48.1 mg, overall yield: 81%, purity: 76%, t_R 11.8 min (analytical HPLC, 10 to 90% acetonitrile in water (0.1% TFA) over 40 min, flow rate of 1.0 mL/min), molecular formula: $C_{20}H_{32}N_6O_6S_2$, calculated mass: 516.1825, found: 516.1783.

23: 52.6 mg, overall yield: 84%, purity: 78%, t_R 12.2 min (analytical HPLC, 10 to 90% acetonitrile in water (0.1% TFA) over 40 min, flow rate of 1.0 mL/min), molecular formula: $C_{22}H_{36}N_6O_6S_2$, calculated mass: 544.2138, found: 544.2164.

24: 61.5 mg, overall yield: 84%, purity: 85%, t_R 15.2 min (analytical HPLC, 10 to 90% acetonitrile in water (0.1% TFA) over 40 min, flow rate of 1.0 mL/min), molecular formula: $C_{27}H_{36}N_6O_8S_2$, calculated mass: 636.2036, found: 636.2058

25: 68.7 mg, overall yield: 92%, purity: 80%, t_R 12.8 (analytical HPLC, 10 to 90% acetonitrile in water (0.1% TFA) over 40 min, flow rate of 1.0 mL/min), molecular formula: $C_{29}H_{43}N_7O_6S_2$, calculated mass: 649.2716, found: 649.2754.

26: 69.1 mg, overall yield: 90%, purity: 81%, t_R 22.6 min (analytical HPLC, 10 to 90% acetonitrile in water (0.1% TFA) over 40 min, flow rate of 1.0 mL/min), molecular formula: $C_{32}H_{40}N_6O_6S_2$, calculated mass: 668.2451, found: 668.2462

27: 56.9 mg, overall yield: 78%, purity: 80%, t_R 22.2 min (analytical HPLC, 10 to 90% acetonitrile in water (0.1% TFA) over 40 min, flow rate of 1.0 mL/min), molecular formula: $C_{29}H_{42}N_6O_6S_2$, calculated mass: 634.2607, found: 634.2634.

28: 58.4 mg, overall yield: 80%, purity: 85%, t_R 22.2 min (analytical HPLC, 10 to 90% acetonitrile in water (0.1% TFA) over 40 min, flow rate of 1.0 mL/min), molecular formula: $C_{29}H_{42}N_6O_6S_2$, calculated mass: 634.2607, found: 634.2634.

29: 58.5 mg, overall yield: 80%, purity: 94%, t_R 22.2 min (analytical HPLC, 10 to 90% acetonitrile in water (0.1% TFA) over 40 min, flow rate of 1.0 mL/min), molecular formula: $C_{22}H_{36}N_6O_6S_2$, calculated mass: 634.2607, found: 634.2594.

30: 55.5 mg, overall yield: 78%, purity: 82%, t_R 18.6 min (analytical HPLC, 10 to 90% acetonitrile in water (0.1% TFA) over 40 min, flow rate of 1.0 mL/min), molecular formula: $C_{28}H_{38}N_6O_6S_2$, calculated mass: 618.2294, found: 618.2254.

31: 61.7 mg, overall yield: 86%, purity: 84%, t_R 19.0 min (analytical HPLC, 10 to 90% acetonitrile in water (0.1% TFA) over 40 min, flow rate of 1.0 mL/min), molecular formula: $C_{32}H_{40}N_6O_7S_2$, calculated mass: 684.2399, found: 684.2420.

32: 70.0 mg, overall yield: 86%, purity: 86%, t_R 19.9 min (analytical HPLC, 10 to 90% acetonitrile in water (0.1% TFA) over 40 min, flow rate of 1.0 mL/min), molecular formula: $C_{34}H_{41}N_7O_6S_2$, calculated mass: 707.2560, found: 707.2587.

33: 67.6 mg, overall yield: 88%, purity: 80%, t_R 23.4 min (analytical HPLC, 10 to 90% acetonitrile in water (0.1% TFA) over 40 min, flow rate of 1.0 mL/min), molecular formula: $C_{32}H_{40}N_6O_6S_2$, calculated mass: 668.2451, found: 668.2488

34: 52.1 mg, overall yield: 75%, purity: 75%, t_R 19.3 min (analytical HPLC, 10 to 90% acetonitrile in water (0.1% TFA) over 40 min, flow rate of 1.0 mL/min), molecular formula: $C_{27}H_{36}N_6O_6S_2$, calculated mass: 604.2138, found: 604.2166.

35: 60.4 mg, overall yield: 82%, purity: 84%, t_R 20.6 min (analytical HPLC, 10 to 90% acetonitrile in water (0.1% TFA) over 40 min, flow rate of 1.0 mL/min), molecular formula: $C_{30}H_{36}N_6O_6S_2$, calculated mass: 640,2138, found: 640.2154

36: 66.7 mg, overall yield: 85%, purity: 80%, t_R 20.7 min (analytical HPLC, 10 to 90% acetonitrile in water (0.1% TFA) over 40 min, flow rate of 1.0 mL/min), molecular formula: $C_{33}H_{42}N_6O_6S_2$, calculated mass: 682.2607, found: 682.2654.

37: 62.8 mg, overall yield: 80%, purity: 85%, t_R 24.4 min (analytical HPLC, 10 to 90% acetonitrile in water (0.1% TFA) over 40 min, flow rate of 1.0 mL/min), molecular formula: $C_{33}H_{42}N_6O_6S_2$, calculated mass: 682.2607, found: 682.2624.

38: 70.0 mg, overall yield: 86%, purity: 82%, t_R 20.8 min (analytical HPLC, 10 to 90% acetonitrile in water (0.1% TFA) over 40 min, flow rate of 1.0 mL/min), molecular formula: $C_{33}H_{42}N_6O_6S_2$, calculated mass: 682.2607, found: 682.2628.

39: 57.5 mg, overall yield: 75%, purity: 80%, t_R 21.7 min (analytical HPLC, 10 to 90% acetonitrile in water (0.1% TFA) over 40 min, flow rate of 1.0 mL/min), molecular formula: $C_{32}H_{38}N_6O_6S_2$, calculated mass: 666.2294, found: 666.2334.

40: 59.0 mg, overall yield: 82%, purity: 85%, t_R 17.5 min (analytical HPLC, 10 to 90% acetonitrile in water (0.1% TFA) over 40 min, flow rate of 1.0 mL/min), molecular formula: $C_{29}H_{34}N_6O_6S_2$, calculated mass: 626.1981, found: 626.1952.

41: 58.7 mg, overall yield: 78%, purity: 78%, t_R 20.2 min (analytical HPLC, 10 to 90% acetonitrile in water (0.1% TFA) over 40 min, flow rate of 1.0 mL/min), molecular formula: $C_{31}H_{36}N_6O_6S_2$, calculated mass: 654.2294, found: 654.2254.

42: 74.1 mg, overall yield: 90%, purity: 85%, t_R 28.7 min (analytical HPLC, 10 to 90% acetonitrile in water (0.1% TFA) over 40 min, flow rate of 1.0 mL/min), molecular formula: $C_{36}H_{40}N_6O_6S_2$, calculated mass: 716.2451, found: 716.2411.

43: 62.2 mg, overall yield: 77%, purity: 77%, t_R 25.0 min (analytical HPLC, 10 to 90% acetonitrile in water (0.1% TFA) over 40 min, flow rate of 1.0 mL/min), molecular formula: $C_{36}H_{38}N_6O_6S_2$, calculated mass: 702.2294, found: 702.2267.

44: 67.6 mg, overall yield: 88%, purity: 88%, t_R 23.4 min (analytical HPLC, 10 to 90% acetonitrile in water (0.1% TFA) over 40 min, flow rate of 1.0 mL/min), molecular formula: $C_{32}H_{40}N_6O_6S_2$, calculated mass: 668.2451, found: 668.2473.

45: 66.2 mg, overall yield: 88%, purity: 86%, t_R 21.2 min (analytical HPLC, 10 to 90% acetonitrile in water (0.1% TFA) over 40 min, flow rate of 1.0 mL/min), molecular formula: $C_{31}H_{38}N_6O_6S_2$, calculated mass: 654.2294, found: 654.2264.

46: 64.0 mg, overall yield: 85%, purity: 84%, t_R 21.0 min (analytical HPLC, 10 to 90% acetonitrile in water (0.1% TFA) over 40 min, flow rate of 1.0 mL/min), molecular formula: $C_{31}H_{38}N_6O_6S_2$, calculated mass: 654.2294, found: 654.2314.

47: 62.6 mg, overall yield: 85%, purity: 85%, t_R 20.6 min (analytical HPLC, 10 to 90% acetonitrile in water (0.1% TFA) over 40 min, flow rate of 1.0 mL/min), molecular formula: $C_{30}H_{36}N_6O_6S_2$, calculated mass: 640,2138, found: 640,2154.

48: 64.3 mg, overall yield: 82%, purity: 92%, t_R 24.0 min (analytical HPLC, 10 to 90% acetonitrile in water (0.1% TFA) over 40 min, flow rate of 1.0 mL/min), molecular formula: $C_{33}H_{42}N_6O_6S_2$, calculated mass: 682.2607, found: 682.2590.

49: 65.9 mg, overall yield: 84%, purity: 88%, t_R 23.7 min (analytical HPLC, 10 to 90% acetonitrile in water (0.1% TFA) over 40 min, flow rate of 1.0 mL/min), molecular formula: $C_{33}H_{42}N_6O_6S_2$, calculated mass: 682.2607, found: 682.2650.

50: 74.5 mg, overall yield: 88%, purity: 92%, t_R 24.2 min (analytical HPLC, 10 to 90% acetonitrile in water (0.1% TFA) over 40 min, flow rate of 1.0 mL/min), molecular formula: $C_{34}H_{44}N_6O_6S_2$, calculated mass: 696.2764, found: 696.2751.

51: 71.0 mg, overall yield: 85%, purity: 85%, t_R 25.7 min (analytical HPLC, 10 to 90% acetonitrile in water (0.1% TFA) over 40 min, flow rate of 1.0 mL/min), molecular formula: $C_{36}H_{42}N_6O_6S_2$, calculated mass: 718.2607, found: 718.2601.

52: 72.3 mg, overall yield: 88%, purity: 80%, t_R 25.3 min (analytical HPLC, 10 to 90% acetonitrile in water (0.1% TFA) over 40 min, flow rate of 1.0 mL/min), molecular formula: $C_{36}H_{42}N_6O_6S_2$, calculated mass: 718.2607, found: 718.2611.

53: 81.3 mg, overall yield: 92%, purity: 90%, t_R 29.4 min (analytical HPLC, 10 to 90% acetonitrile in water (0.1% TFA) over 40 min, flow rate of 1.0 mL/min), molecular formula: $C_{40}H_{44}N_6O_6S_2$, calculated mass: 768.2764, found: 768.2798.

54: 79.5 mg, overall yield: 90%, purity: 88%, t_R 28.9 min (analytical HPLC, 10 to 90% acetonitrile in water (0.1% TFA) over 40 min, flow rate of 1.0 mL/min), molecular formula: $C_{40}H_{44}N_6O_6S_2$, calculated mass: 768.2764, found: 768.2734.

55: 72.4 mg, overall yield: 86%, purity: 92%, t_R 27.3 min (analytical HPLC, 10 to 90% acetonitrile in water (0.1% TFA) over 40 min, flow rate of 1.0 mL/min), molecular formula: $C_{37}H_{44}N_6O_6S_2$, calculated mass: 732.2764, found: 732.2743.

56: 77.2 mg, overall yield: 90%, purity: 90%, t_R 22.5 min (analytical HPLC, 10 to 90% acetonitrile in water (0.1% TFA) over 40 min, flow rate of 1.0 mL/min), molecular formula: $C_{36}H_{42}N_7O_6S_2$, calculated mass: 746.2669, found: 746.2698.

57: 83.0 mg, overall yield: 88%, purity: 82%, t_R 27.7 min (analytical HPLC, 10 to 90% acetonitrile in water (0.1% TFA) over 40 min, flow rate of 1.0 mL/min), molecular formula: $C_{44}H_{48}N_6O_6S_2$, calculated mass: 820.3077, found: 820.3112

58: 69.4 mg, overall yield: 88%, purity: 87%, t_R 23.5 min (analytical HPLC, 10 to 90% acetonitrile in water (0.1% TFA) over 40 min, flow rate of 1.0 mL/min), molecular formula: $C_{32}H_{39}FN_6O_6S_2$, calculated mass: 686.2357, found: 686.2320.

59: 67.1 mg, overall yield: 85%, purity: 85%, t_R 22.8 min (analytical HPLC, 10 to 90% acetonitrile in water (0.1% TFA) over 40 min, flow rate of 1.0 mL/min), molecular formula: $C_{32}H_{39}FN_6O_6S_2$, calculated mass: 686.2357, found: 686.2390.

60: 73.8 mg, overall yield: 90%, purity: 94%, t_R 22.5 min (analytical HPLC, 10 to 90% acetonitrile in water (0.1% TFA) over 40 min, flow rate of 1.0 mL/min), molecular formula: $C_{32}H_{39}N_7O_8S_2$, calculated mass: 713.2303, found: 713.2287.

61: 75.5 mg, overall yield: 92%, purity: 81%, t_R 22.8 min (analytical HPLC, 10 to 90% acetonitrile in water (0.1% TFA) over 40 min, flow rate of 1.0 mL/min), molecular formula: $C_{32}H_{39}N_7O_8S_2$, calculated mass: 713.2303, found: 713.2343.

62: 82.8 mg, overall yield: 92%, purity: 84%, t_R 29.7 min (analytical HPLC, 10 to 90% acetonitrile in water (0.1% TFA) over 40 min, flow rate of 1.0 mL/min), molecular formula: $C_{41}H_{46}N_6O_6S_2$, calculated mass: 782.2920, found: 782.2954

8. References

1.   Bishop, J.M. and Weinberg, R.A., eds. (1996). Molecular Oncology In Cancer Medicine (New York: Scientific American, Inc.).

2.   Hanahan D. and Weinberg R.A. The Hallmarks of Cancer. *Cell.* **2000,** *100***,** 57–70.

3.   Fedi, P., Tronick, S.R., and Aaronson, S.A. (1997). Growth factors In Cancer Medicine, J.F. Holland, R.C. Bast, D.L. Morton, E. Frei, D.W. Kufe, and R.R. Weichselbaum, eds. (Baltimore, MD: Williams and Wilkins), pp. 41–64.

4.   (a) Giancotti, F.G., and Ruoslahti, E. Integrin signaling. *Science* **1999**, *285*, 1028–1032. (b) Lukashev, M.E., and Werb, Z. ECM signaling: orchestrating cell behavior and misbehaviour. *Trends Cell Biol.* **1998**, *8*, 437–441.

5.   Medema, R.H., and Bos, J.L. The role of p21-ras in receptor tyrosine kinase signaling. *Crit. Rev. Oncog.* **1993**, *4*, 615–661.

6.   Downward, J. Mechanisms and consequences of activation of protein kinase B/Akt. *Curr. Opin. Cell Biol.* **1998**, *10*, 262–267.

7.   (a) Skobe, M., and Fusenig, N.E. Tumorigenic conversion of immortal human keratinocytes through stromal cell activation. *Proc. Natl. Acad. Sci.* USA **1998**, *95*, 1050–1055. (b) Kinzler, K.W., and Vogelstein, B. Landscaping the cancer in human cancer terrain. *Science* **1998**, *280*, 1036–1037. (c) Olumi, A.F., Grossfeld, G.D., Hayward, S.W., Carroll, P.R., Tlsty, T.D. and Cunha, G.R. Carcinoma-associated fibroblasts direct tumor progression of initiated human prostatic epithelium. *Cancer Res.* **1999**, *59*, 5002–5011.

8.   Weinberg, R.A. The retinoblastoma protein and cell cycle control. *Cell* **1995**, *81*, 323-330.

9.   Fynan, T.M., and Reiss, M. Resistance to inhibition of cell growth by transforming growth factor-b and its role in oncogenesis. *Crit. Rev. Oncog.* **1993**, *4*, 493–540.

10.   (a) Foley, K.P., and Eisenman, R.N. Two MAD tails: what the recent knockouts of Mad1 and Mx1 tell us about the MYC/MAX/ MAD network. *Biochim. Biophys. Acta* **1999**, *1423*, M37–47. (b) Kinzler, K.W., and Vogelstein, B. Lessons from hereditary colorectal cancer. *Cell.* **1996**, *87*, 159–170.

11.   (a) Butt, A.J., Firth, S.M., and Baxter, R.C. The IGF axis and programmed cell death. *Immunol. Cell Biol.* **1999**, *77*, 256–262. (b) Lotem, J., and Sachs, L. Control of apoptosis in hematopoiesis and leukemia by cytokines, tumor suppressor and oncogenes. *Leukemia* **1999**, *10*, 925–931.

12.   Evan, G., and Littlewood, T. A matter of life and cell death. *Science* **1998**, *281*, 1317–1322.

13.   Thornberry, N.A., and Lazebnik, Y. Caspases: enemies within. *Science* **1998**, *281*, 1312–16.

14.   Harris, C.C. p53 tumor suppressor gene: from the basic research laboratory to the clinic-an abridged historical perspective. *Carcinogenesis* **1996**, *17*, 1187–1198.

15.   Hayflick, L. Mortality and immortality at the cellular level. A review. *Biochemistry* **1997**, *62*, 1180–1190.

16.   Counter, C.M., Avilion, A.A., LeFeuvre, C.E., Stewart, N.G., Greider, C.W., Harley, C.B., and Bacchetti, S. Telomere shortening chromosome instability is arrested in immortal cells which express telomerase activity. *EMBO J.* **1992**, *11*, 1921–1929.

17.   Shay, J.W., and Bacchetti, S. A survey of telomerase activity in human cancer. *Eur. J. Cancer* **1997**, *33*, 787–791.

18.   (a) Bodnar, A.G., Ouellete, M., Frolkis, M., Holt, S.E., Chiu, C., Morin, G.B., Harley, C.B., Shay, J.W., Lichtsteiner, S., and Wright, W.E. Extension of life-span by introduction of telomerase into normal human cells. *Science* **1998**, *279*, 349–352. (b) Counter, C.M., Hahn, W.C., Wei, W., Dickinson Caddle, S., Beijers-bergen, R.L., Lansdorp, P.M., Sedivy, J.M., and Weinberg, R.A. Dissociation between telomerase activity, telomere maintenance and cellular immortalization. *Proc. Natl. Acad. Sci. USA* **1998**, *95*, 14723–14728. (c) Greenberg, R.A., Chin, L., Femino, A., Lee, K.H., Gottlieb, G.J., Singer, R.H., Greider, C.W., and DePinho, R.A. Short dysfunctional telomeres impair tumorigenesis in the INK4aD2/3 cancer-prone mouse. *Cell* **1999**, *97*, 515–525.

19.   Veikkola, T., and Alitalo, K. VEGFs, receptors and angiogenesis. *Semin. Cancer Biol.* **1999**, *9*, 211–220.

20.   (a) Varner, J.A., and Cheresh, D.A. Integrins and cancer. *Curr. Opin. Cell Biol.* **1996**, *8*, 724–730. (b) Hynes, R.O., and Wagner, D.D. Genetic manipulation of vascular adhesion molecules in mice. *J. Clin. Invest.* **1996**, *98*, 2193–2195.

21.   (a) Bouck, N., Stellmach, V., and Hsu, S.C. How tumors become angiogenic. *Adv. Cancer Res.* **1996**, *69*, 135–174. (b) Folkman, J. (1997). Tumor angiogenesis. In Cancer Medicine, J.F. Holland, R.C. Bast, D.L. Morton, E. Frei, D.W. Kufe, and R.R. Weich- R.R. eds. (Baltimore, MD: Williams and Wilkins), pp. 181–204.

22.   (a) Singh, R.K., Gutman, M., Bucana, C.D., Sanchez, R., Llansa, N., and Fidler, I.J. Interferons alpha and beta down-regulate the expression of basic fibroblast growth factor in human carcinomas. *Proc. Natl. Acad. Sci. USA* **1995**, *92*, 4562–

4566. (b) Volpert, O.V., Dameron, K.M., and Bouck, N. Sequential development of an angiogenic phenotype by human fibroblasts progressing to tumorigenicity. *Oncogene* **1997**, *14*, 1495–1502.

23.   Rak, J., Filmus, J., Finkenzeller, G., Grugel, S., Marme, D., and Kerbel, R.S. Oncogenes   as inducers of tumor angiogenesis. *Cancer Metastasis Rev.* **1995**, *14*, 263–277.

24.   (a) Johnson, J.P. Cell adhesion molecules of the immunoglobulin supergene family and their role in malignant transformation and progression to metastatic disease. *Cancer Metastasis   Rev.* **1991**, *10*, 11–22. (b) Kaiser, U., Auerbach, B., and Oldenburg, M. The neural cell   adhesion   molecule   NCAM   in   multiple myeloma. *Leuk. Lymphoma* **1996**, *20*, 389–395.

25.   Coussens, L.M., and Werb, Z. Matrix metalloproteinases and the development of cancer. *Chem. Biol.* **1996**, *3*, 895–904.

26.   Stetler-Stevenson, W.G. Matrix metalloproteinases in angiogenesis: a moving target for therapeutic intervention. *J. Clin. Invest.* **1999**, *103*, 1237–1241.

27.   Werb, Z. ECM and cell surface proteolysis: regulating cellular ecology. *Cell* **1997** *91*, 439–442.

28.   (a) Lund, A. H. & van Lohuizen, M. Epigenetics and cancer. *Genes Dev.***2004**, *18*, 2315– 2335. (b) Baylin, S. B. & Ohm, J. E. Epigenetic gene silencing in cancer- a mechanism for early oncogenic pathway addiction? *Nature Rev. Cancer* **2006**, *6*, 107–116.

29.   Pandolfi, P. P. Histone deacetylases and   transcriptional   therapy   with   their inhibitors. *Cancer Chemother. Pharmacol.* **2001***, 48* (Suppl. 1), S17–S19.

30. (a) Nightingale, K. P., O'Neill, L. P. & Turner, B. M. Histone modifications: signaling receptors and potential elements of a heritable epigenetic code. *Curr. Opin. Genet. Dev.* **2006**, *16*, 125–136. (b) Roth, S. Y., Denu, J. M. & Allis, C. D. Histone acetyltransferases. *Annu. Rev. Biochem.* **2001**, *70*, 81–120.

31. Kouzarides, T. Chromatin modifications and their function. *Cell* **2007**, *128*, 693–705.

32. (a) Shogren-Knaak, M. et al. Histone H4-K16 acetylation controls chromatin structure and protein interactions. *Science* **2006**, *311*, 844–847.(b) Shogren-Knaak, M. and Peterson, C.L. Switching on chromatin: mechanistic role of histone H4-K16 acetylation. *Cell Cycle* **2006**, *5*, 1361–1365.

33. (a) Jenuwein, T. and Allis, C.D. Translating the histone code. *Science* **2001**, *293*, 1074– 1080. (b) Shi, Y. and Whetstine, J.R. Dynamic regulation of histone lysine methylation by demethylases. *Mol. Cell* **2007**, *25*, 1–14.

34. Marks, P. et al. Histone deacetylases and cancer: causes and therapies. Nat. Rev. Cancer **2001**, *1*, 194–202.

35. (a) George, P. *et al*. Combination of the histone deacetylase inhibitor LBH589 and the hsp90 inhibitor 17-AAG is highly active against human CML-BC cells and AML cells with activating mutation of FLT-3. *Blood* **2005**, *105*, 1768–1776. (b) Rahmani, M. *et al*. Coadministration of the heat shock protein 90 antagonist 17-allylamino- 17-demethoxygeldanamycin with suberoylanilide hydroxamic acid or sodium butyrate synergistically induces apoptosis in human leukemia cells. *Cancer Res.* **2003**, *63*, 8420– 8427.

36. Yang, X.J. The diverse superfamily of lysine acetyltransferases and their roles in leukemia and other diseases. Nucleic Acids Res. **2004**, *32*, 959–976.

37.   Johnstone, R. W. Histone-deacetylase inhibitors : novel drugs for the treatment of cancer. *Nat. Rev. Drug Discovery* **2002**, *1*, 287-299.

38.   (a) Fischle, W., Dequiedt, F., Fillion, M., Hendzel, M. J., Voelter, W. and Verdin, E. Human HDAC7 histone deacetylase activity is associated with HDAC3 in vivo. *J. Biol. Chem.* **2001**, *276*, 35826-35835. (b) Yang, W. M., Tsai, S. C., Wen, Y. D., Fejer, G. and Seto, E. Functional domains of histone deacetylase-3. *J. Biol. Chem.* **2002**, *277*, 9447-9454.

39.   Van den Wyngaert, I., de Vries, W., Kremer, A., Neefs, J., Verhasselt, P., Luyten, W. H. and Kass, S. U. Cloning and characterization of human histone deacetylase 8. *FEBS Lett.* **2000**, *478*, 77-83.

40.   Kao, H. Y., Downes, M., Ordentlich, P. and Evans, R. M. Isolation of a novel histone deacetylase reveals that class I and class II deacetylases promote SMRT-mediated repression. *Genes Dev*. **2000**, *14*, 55-66.

41.   Guenther, M. G., Barak, O. and Lazar, M. A.(2001) The SMRT and N-CoR corepressors are activating cofactors for histone deacetylase 3. *Mol. Cell. Biol.* **2001**, *21*, 6091-6101.

42.   (a) Buggy, J. J., Sideris, M. L., Mak, P., Lorimer, D. D., McIntosh, B. and Clark, J. M. Cloning and characterization of a novel human histone deacetylase, HDAC8. *Biochem. J.* **2000**, *350*, 199-205. (b) Hu, E., Chen, Z., Fredrickson, T., Zhu, Y., Kirkpatrick, R., Zhang, G. F., Johanson, K., Sung, C. M., Liu, R. and Winkler, J. Cloning and characterization of a novel human class I histone deacetylase that functions as a transcription repressor. *J. Biol. Chem.* **2000**, *275*, 15254-15264.

43.   (a) Bertos, N. R., Wang, A. H. and Yang, X. J. Class II histone deacetylases : structure, function, and regulation. *Biochem. Cell Biol.* **2001**, *79*, 243-252. (b)

Zhou, X., Marks, P. A., Rifkind, R. A. and Richon, V. M. Cloning and characterization of a histone deacetylase, HDAC9. *Proc. Natl. Acad. Sci. U.S.A.* **2001**, *98*, 10572-10577.

44.   McKinsey, T. A., Zhang, C. L. and Olson, E. N. Control of muscle development by dueling HATs and HDACs. *Curr. Opin. Genet. Dev.* **2001**, *11*, 497-504.

45.   Wade, P. A. Transcriptional control at regulatory checkpoints by histone deacetylases : molecular connections between cancer and chromatin. *Hum. Mol. Genet.* **2001**, *10*, 693-698.

46.   (a) Kao, H. Y., Verdel, A., Tsai, C. C., Simon, C., Juguilon, H. and Khochbin, S. Mechanism for nucleocytoplasmic shuttling of histone deacetylase 7. *J. Biol. Chem.* **2001**, *276*, 47496-47507. (b) Dressel, U., Bailey, P. J., Wang, S. C., Downes, M., Evans, R. M.   and Muscat, G. E. A dynamic role for HDAC7 in MEF2-mediated muscle diåerentiation. *J. Biol. Chem.* **2001**, *276*, 17007-17013.

47.   (a) Fischle, W., Dequiedt, F., Fillion, M., Hendzel, M. J., Voelter, W. and Verdin, E. Human HDAC7 histone deacetylase activity is associated with HDAC3 in vivo. *J. Biol. Chem.* **2001**, *276*, 35826-35835. (b) Yang, W. M., Tsai, S. C., Wen, Y. D., Fejer, G. and Seto, E. Functional domains of histone deacetylase-3. *J. Biol. Chem.* **2002**, *277*, 9447-9454.

48.   Zhou, X., Richon, V. M., Rifkind, R. A. and Marks, P. A. Identification of a transcriptional repressor related to the noncatalytic domain of histone deacetylases 4 and 5. *Proc. Natl. Acad. Sci. U.S.A.* **2000**, *97*, 1056-1061.

49.   (a) Hubbert, C., Guardiola, A., Shao, R., Kawaguchi, Y., Ito, A., Nixon, A., Yoshida, M., Wang, X. F. and Yao, T. P. HDAC6 is a microtubule-associated deacetylase. *Nature   (London)* **2002**, *417*, 455-458. (b) Fischer, D. D., Cai, R.,

Bhatia, U., Asselbergs, F. A., Song, C., Terry, R., Trogani, N., Widmer, R., Atadja, P. and Cohen, D. Isolation and characterization of a novel class II histone deacetylase, HDAC10. *J. Biol. Chem.* **2002**, *277,* 6656-6666.

50.   (a) Marks, P., Rifkind, R. A., Richon, V. M., Breslow, R., Miller, T. and Kelly, W. K. Histone deacetylases and cancer : causes and therapies. *Nat. Rev. Cancer* 2001, *1,* 194-202. (b) Yoshida, M., Furumai, R., Nishiyama, M., Komatsu, Y., Nishino, N. and Horinouchi, S. Histone deacetylase as a new target for cancer chemotherapy. *Cancer Chemother. Pharmacol.* **2001**, *48* (Suppl. 1), S20-S26.

51.   (a) Guardiola, A. R. and Yao, T. P. Molecular cloning and characterization of a novel histone deacetylase HDAC10. *J. Biol. Chem.* **2002**, *277*, 3350-3356. (b) Tong, J. J., Liu, J.,   Bertos, N. R. and Yang, X. J. Identification of HDAC10, a novel class II human histone deacetylase containing a leucine-rich domain. *Nucleic Acids Res.* **2002**, *30*, 1114-1123.

52.   Gao, L., Cueto, M. A., Asselbergs, F. and Atadja, P. Cloning and functional characterization of HDAC11, a novel member of the human histone deacetylase family. *J. Biol. Chem.* **2002**, *277*, 25748-25755.

53.   Finnin M. S., Donigian J. R., Pavletich N. P. Structure of the histone deacetylase SIRT2. *Nat. Struct. Biol.* **2001***, 8*, 621-625.

54.   North B. J. and Verdin E. Sirtuins: Sir2-related NAD-dependent protein deacetylases. *Genome Biology* **2004**, *5***,** 224.4-224.12.

55.   (a) Cote, S. *et al*. Response to histone deacetylase inhibition of novel PML/RARα mutants detected in retinoic acid-resistant APL cells. *Blood* **2002**, *100*, 2586–2596. (b) He, L. Z. *et al*. Histone deacetylase inhibitors induce remission in

transgenic models of therapy-resistant acute promyelocytic leukemia. *J. Clin. Invest.* **2001**, *108*, 1321–1330.

56. Pasqualucci, L. *et al*. Molecular pathogenesis of non- Hodgkin's lymphoma: the role of Bcl-6. *Leuk. Lymphoma* **2003**, *44* (Suppl. 3), S5–S12.

57. Halkidou, K. *et al*. Upregulation and nuclear recruitment of HDAC1 in hormone refractory prostate cancer. *Prostate* **2004**, *59*, 177–189.

58. Choi, J. H. *et al*. Expression profile of histone deacetylase 1 in gastric cancer tissues. *Jpn J. Cancer Res.* **2001**, *92*, 1300–1304.

59. Wilson, A. J. *et al*. Histone deacetylase 3 (HDAC3) and other class I HDACs regulate colon cell maturation and p21 expression and are deregulated in human colon cancer. *J. Biol. Chem.* **2006**, *281*, 13548–13558.

60. Zhang, Z. *et al*. Quantitation of HDAC1 mRNA expression in invasive carcinoma of the breast. *Breast Cancer Res. Treat* **2005**, *94*, 11–16.

61. Zhu, P. *et al*. Induction of HDAC2 expression upon loss of APC in colorectal tumorigenesis. *Cancer Cell* **2004**, *5*, 455–463.

62. Huang, B. H. *et al*. Inhibition of histone deacetylase 2 increases apoptosis and p21Cip1/WAF1 expression, independent of histone deacetylase 1. *Cell Death Differ.* **2005**, *12*, 395–404.

63. Song, J. *et al*. Increased expression of histone deacetylase 2 is found in human gastric cancer. *APMIS* **2005**, *113*, 264–268.

64. Zhang, Z. *et al*. HDAC6 expression is correlated with better survival in breast cancer. *Clin. Cancer Res.* **2004**, *10*, 6962–6968.

65. Drummond, D. C. *et al*. Clinical development of histone deacetylase inhibitors as anticancer agents. *Annu. Rev. Pharmacol. Toxicol.* **2005**, *45*, 495–528.

66. Dokmanovic, M. & Marks, P. A. Prospects: histone deacetylase inhibitors. *J. Cell. Biochem.* **2005**, *96*, 293–304.

67. Kelly, W. K. & Marks, P. A. Drug insight: Histonedeacetylase inhibitors-development of the   new targeted anticancer agent suberoylanilide hydroxamic acid. *Nature Clin. Pract. Oncol.* **2005**, *2*, 150–157.

68. (a) Johnstone, R. W. Histone-deacetylase inhibitors: novel drugs for the treatment of cancer. *Nature Rev. Drug Discov.* 2002, *1*, 287–299. (b) Minucci, S. & Pelicci, P. G. Histone deacetylase inhibitors and the promise of epigenetic (and more) treatments for cancer. *Nature Rev. Cancer* **2006**, *6*, 38–51.

69. Insinga, A. *et al*. Inhibitors of histone deacetylases induce tumor-selective apoptosis through activation of the death receptor pathway. *Nature Med.* **2005**, *11*, 71–76.

70. Willis, S. N. & Adams, J. M. Life in the balance: howBH3-only proteins induce apoptosis. *Curr. Opin. Cell. Biol.* **2005***, 17*, 617–625.

71. Ruefli, A. A. *et al*. The histone deacetylase inhibitor and chemotherapeutic agent suberoylanilide hydroxamic acid (SAHA) induces a cell-death pathway characterized by cleavage of Bid and production of reactive oxygen species. *Proc. Natl Acad. Sci. USA* **2001***,   98*, 10833–10838.

72. Rosato, R. R., Almenara, J. A. & Grant, S. The histone deacetylase inhibitor MS-275 promotes differentiation or apoptosis in human leukemia cells through a process regulated by generation of reactive oxygen species and induction of p21CIP1/WAF1 1. *Cancer Res.* **2003**, *63*, 3637–3645.

73. (a) Johnstone, R. W. Histone-deacetylase inhibitors: novel drugs for the treatment of cancer. *Nature Rev. Drug Discov.* **2002***, 1*, 287–299. (b) Marks, P. A., Miller, T.and Richon, V. M. Histone deacetylases. *Curr. Opin. Pharmacol.* **2003***, 3*, 344–351 (2003).

74. Haggarty, S. J., Koeller, K. M., Wong, J. C., Grozinger, C. M. & Schreiber, S. L. Domain-selective smallmolecule inhibitor of histone deacetylase 6 (HDAC6)-mediated tubulin deacetylation. *Proc. Natl Acad. Sci. USA* **2003***,100*, 4389–4394.

75. Vrana, J. A. *et al*. Induction of apoptosis in U937 human leukemia cells by suberoylanilide hydroxamic acid (SAHA) proceeds through pathways that are regulated by Bcl-2/Bcl-XL, c-Jun, and p21CIP1, but independent of p53. *Oncogene* **1999**, *18,* 7016–7025.

76. Glaser, K. B. *et al*. Gene expression profiling of multiple histone deacetylase (HDAC) inhibitors: defining a common gene set produced by HDAC inhibition in T24 and MDA carcinoma cell lines. *Mol. Cancer Ther.* **2003**, *2*, 151–163.

77. Chen, Z. *et al*. Induction and superinduction of growth arrest and DNA damage gene 45 (GADD45) α and β messenger RNAs by histone deacetylase inhibitors trichostatin A (TSA) and butyrate in SW620 human colon carcinoma cells. *Cancer Lett.* **2002**, *188*, 127–140**.**

78.   Qiu, L. *et al*. Histone deacetylase inhibitors trigger a G2 checkpoint in normal cells that is defective in tumor cells. *Mol. Biol. Cell.* **2000**, *11*, 2069–2083.

79.   (a) Pili, R., Kruszewski, M. P., Hager, B. W., Lantz, J. & Carducci, M. A. Combination of phenylbutyrate and 13-cis retinoic acid inhibits prostate tumor growth and   angiogenesis. *Cancer Res.* **2001**, *61*, 1477–1485; (b) Sasakawa, Y. *et al*. Antitumor efficacy of FK228, a novel histone deacetylase inhibitor, depends on the effect on expression of angiogenesis factors. *Biochem. Pharmacol.* **2003**, *66*, 897–906; (c) Michaelis, M. *et al*. Valproic acid inhibits angiogenesis *in vitro* and *in vivo*. *Mol. Pharmacol.* **2004**, *65*, 520–527 (2004); (d) Rossig, L. *et al*. Inhibitors of histone deacetylation downregulate the expression of endothelial nitric oxide synthase and compromise endothelial cell function in vasorelaxation and angiogenesis. *Circ. Res.* **2002**, *91*, 837–844.

80.   Qian, D. Z. *et al*. Targeting tumor angiogenesis with histone deacetylase inhibitors: the hydroxamic acid derivative LBH589. *Clin. Cancer Res.* **2006**, *12*, 634–642.

81.   (a) Kim, S. H. *et al*. Apicidin is a histone deacetylase inhibitor with anti-invasive and   anti-angiogenic potentials. *Biochem. Biophys. Res. Commun.* **2004**, *315*, 964– 970;   (b) Liu, L. T., Chang, H. C., Chiang, L. C. & Hung, W. C. Histone deacetylase   inhibitor up-regulates RECK to inhibit MMP-2 activation and cancer cell invasion. *Cancer Res.* **2003**, *63*, 3069–3072; (c) Klisovic, D. D. *et al*. Depsipeptide inhibits migration of primary and metastatic uveal melanoma cell lines *in vitro*: a potential strategy for uveal melanoma. *Melanoma Res.* **2005**, *15*, 147–153.

82.   (a) Maeda, T., Towatari, M., Kosugi, H. & Saito, H. Up-regulation of costimulatory/adhesion molecules by histone deacetylase inhibitors in acute myeloid leukemia cells. *Blood* **2000**, *96*, 3847–3856; (b) Magner, W. J. *et al*. Activation of MHC class I, II, and CD40 gene expression by histone deacetylase inhibitors. *J. Immunol.* **2000**, *165*, 7017–7024.

83.   (a) Armeanu, S. *et al*. Natural killer cell-mediated lysis of hepatoma cells via specific induction of NKG2D ligands by the histone deacetylase inhibitor sodium valproate. *Cancer Res.* **2005**, *65*, 6321–6329; (b) Skov, S. *et al*. Cancer cells become susceptible to natural killer cell killing after exposure to histone deacetylase inhibitors due to glycogen synthase   kinase-3-dependent expression of MHC class I-related chain A and B. *Cancer Res.* **2005**, *65*, 11136–11145.

84.   Reddy, P. *et al*. Histone deacetylase inhibitor suberoylanilide hydroxamic acid reduces acute graftversus- host disease and preserves graft-versusleukemia effect. *Proc. Natl Acad. Sci. USA* **2004**, *101*, 3921–3926 (2004).

87.   Pediconi, N. *et al*. Differential regulation of E2F1 apoptotic target genes in response to DNA damage. *Nature Cell Biol.* **2003**, *5*, 552–558.

88.   (a) Chipuk, J. E. & Green, D. R. Dissecting p53-dependent apoptosis. *Cell Death Differ.* **2006**, *13*, 994–1002. (b) Tomita, Y. *et al*. WTp53 but not tumor-derived mutants bind to BCL2 via the DNA binding domain and induce mitochondrial permeabilization. *J. Biol. Chem.* **2006**, *281*, 8600–8606.

89.   Xu, Y. Regulation of p53 responses by posttranslational modifications. *Cell Death Differ.* **2003**, *10*, 400–403.

90. Blagosklonny, M. V. *et al.* Depletion of mutant p53 and cytotoxicity of histone deacetylase inhibitors. *Cancer Res.* **2005**, *65*, 7386–7392.

91. (a) Chen, C., Edelstein, L. C. & Gelinas, C. The Rel/NF-κB family directly activates expression of the apoptosis inhibitor Bcl-x(L). *Mol. Cell Biol.* **2000**, *20*, 2687–2695. (b) Stehlik, C. *et al.* Nuclear factor (NF)-κB-regulated X-chromosome-linked iap gene expression protects endothelial cells from tumor necrosis factor α-induced apoptosis. *J. Exp. Med.* **1998**, *188*, 211–26.

92. Glozak, M. A., Sengupta, N., Zhang, X. & Seto, E. Acetylation and deacetylation of non-histone proteins. *Gene* **2005**, *363*, 15–23.

93. (a) Cohen, H. Y. *et al.* Acetylation of the C terminus of Ku70 by CBP and PCAF controls Bax-mediated apoptosis. *Mol. Cell* **2004**, *13*, 627–638. (b) Subramanian, C., Opipari, A. W., Jr., Bian, X., Castle, V. P. & Kwok, R. P. Ku70 acetylation mediates neuroblastoma cell death induced by histone deacetylase inhibitors. *Proc. Natl Acad. Sci. USA* **2005**, *102*, 4842–4847.

94. (a) Canettieri, G. *et al.* Attenuation of a phosphorylationdependent activator by an HDAC-PP1 complex. *Nature Struct. Biol.* **2003**, *10,* 175–181. (b) Brush, M. H., Guardiola, A., Connor, J. H., Yao, T. P. & Shenolikar, S. Deactylase inhibitors disrupt cellular complexes containing protein phosphatases and deacetylases. *J. Biol. Chem.* **2004**, *279*, 7685–7691. (c) Chen, C. S., Weng, S. C., Tseng, P. H. & Lin, H. P. Histone acetylation-independent effect of histone deacetylase inhibitors on Akt through the reshuffling of protein phosphatase 1 complexes. *J. Biol. Chem.* **2005**, *280*, 38879–38887.

95. Whitesell, L. & Lindquist, S. L. HSP90 and the chaperoning of cancer. *Nature Rev. Cancer* **2005**, *5*, 761–772.

96. Bali, P. *et al*. Inhibition of histone deacetylase 6 acetylates and disrupts the chaperone function of heat shock protein 90: a novel basis for antileukemia activity of histone deacetylase inhibitors. *J. Biol. Chem.* **2005**, *280*, 26729–26734.

97. Bolden J. E.; Peart M. J. and Johnstone R. W. Anticancer activities of histone deacetylase inhibitors. *Nature Rev. Drug Discovery* **2006**, *5*, 769-784

98. (a) Leder, A.; Orkin, S. & Leder, P. Differentiation of erythroleukemic cells in the presence of inhibitors of DNA synthesis. *Science* **1975**, *190*, 893–894. (b) Riggs, M. G.; Whittaker, R. G.; Neumann, J. R. & Ingram, V. M. n-Butyrate causes histone modification in HeLa and Friend erythroleukaemia cells. *Nature* **1977**, *268*, 462–464.

99. Aihua, X.; Chenzhong, L.; Zhibin, L.; Zhiqiang, N.; Weiming, H.; Xianping, L.; Leming, S.; Jiaju, Z. Quantitative Structure-Activity Relationship Study of Histone Deacetylase Inhibitors. *Curr. Med. Chem. Anti-Cancer Agents* **2004**, *4*, 273-299.

100. Curtin, M.; Glaser, K. Histone deacetylase inhibitors: the abbott experience. *Curr. Med. Chem.* **2003**, *10,* 2373-2392.

101. Fujisawa Pharmaceutical Co., Ltd., Jpn. Kokai Tokkyo Koho JP, 03141296 (**1991**).

102. Furumai, R.; Matsuyama, A.; Kobashi, N.; Lee, K.; Nishiyama, M.; Nakajima, H.; Tanaka, A.; Komatsu, Y.; Nishino, N.; Yoshida, M; Horinouchi, S. FK228

(Depsipeptide) as a Natural Prodrug That Inhibits Class I Histone Deacetylases. *Cancer Res*. **2002**, *62*, 4916-4921.

103. Hassig, C. A.; Schreiber, S. L. Nuclear histone acetylases and deacetylases and transcriptional regulation: HATS off to HDACs. *Curr. Opin. Chem. Biol*. **1997**, *1*, 300-308.

104. Curtin, M.; Glaser, K. Histone deacetylase inhibitors: the abbott experience. *Curr. Med. Chem*. **2003**, *10,* 2373-2392.

105. Li, K.; Wu, J.; Xing, W.; Simon, J. A. Total Synthesis of the Antitumor Depsipeptide FR-901-228. *J. Am. Chem. Soc*. **1996**, *118*, 7237-7238.

106. Greshock, T. J.; Johns, D. M.; Noguchi, Y.; Williams, R. M. Improved Total Synthesis of the Potent HDAC Inhibitor FK228 (FR-901228). *Org. Lett*. **2008**, *10*, 613-616.

107. Di Maro S.; Pong R.-C.; Hsieh J.-T; Ahn J.-M. Efficient Solid-Phase Synthesis of FK228 Analogues as Potent Antitumoral Agents. *J. Med. Chem*. **2008**, *51*, 6639-6641.

108. (a) Ahn, J.-M.; Boyle, N. A.; MacDonald, M. T.; Janda, K. D. Peptidomimetics and Peptide Backbone Modifications. *Mini-Rev. Med. Chem.* **2002**, *2*, 463-473; (b) Hruby, V. J.; Ahn, J.-M.; Liao, S. Synthesis of Oligopeptide and Peptidomimetic Libraries. *Curr. Opin. Chem. Biol.* **1997**, *1*, 114-119.

109. Otrubova K.; Lushington G.; Vander Velde D.; McGuire K. L.; McAlpine S. R. Comprehensive Study of Sansalvamide A Derivatives and their Structure-Activity

Relationships against Drug-Resistant Colon Cancer Cell Lines. *J. Med. Chem.* **2008**, *51*, 530-544.

110. Mohamadi, F.; Richards, N. G. J.; Guida, W. C.; Liskamp, R.; Lipton, M.; Caufield, C.; Chang, G.; Hendrickson, T.; Still, W. C. Macromodel - an Integrated Software System for Modeling Organic and Bioorganic Molecules using Molecular Mechanics. *J. Comput. Chem.* **1990**, *11*, 440-467.

111. (a) Jensen, K. J.; Alsina, J.; Songster, M. F.; Vagner, J.; Albericio, F.; Barany, G. Backbone Amide Linker (BAL) Strategy for Solid-Phase Synthesis of C-Terminal-Modified and Cyclic Peptides. *J. Am. Chem. Soc.* **1998**, *120*, 5441-5452. (b) Guillaumie F.; Kappel J. C.; Kelly N. M.; Barany. G. and Jensen K. J.Solid-Phase synthesis of C-teriman Peptide Aldehyde from Amino Acetals Anchored to a Backbone Amide Linker (BAL) handle. Tetrahedron Lett. **2000**, *41*, 6131-6135.

112. Knorr R., Trzeciak, A.; Bannwarth W.; Gillessen D.; *Tetrahedron Lett.,* **1989***, 30,* 1927-1930.

113. Carpino, L.A.; El-Faham, A. *J. Am. Chem. Soc.* **1995**, *117*, 5401.

114. Karam, J. A.; Fan, J.; Stanfield, J.; Richer, E.; Benaim, E. A.; Frenkel, E. P.; Sagalowsky, A. I.; Antich, P. P.; Mason, R. P.; Hsieh, J.-T. The use of histone deacetylase inhibitor FK228 and DNA hypomethylation agent 5-Azacytidine in human bladder cancer therapy. *Int. J. Cancer* **2007**, *120*, 1795-1802.

115. Kaiser, E.; Colescott, R. L.; Bossinger, C. D.; Cook, P. I. Color test for detection of free terminal amino groups in the solid-phase synthesis of peptides. *Anal. Biochem.* **1970**, *34*, 595-598.

116.   Hancock, W. S.; Battersby, J.E. A new micro-test for the detection of incomplete coupling reactions in solid-phase peptide synthesis using 2,4,6-trinitrobenzenesulphonic acid. *Anal. Biochem.* **1976**, *71*, 260-264.

117.   Vojkovsky, T.. Detection of secondary amines on solid phase. *Pept Res.* 1995, 8, 236-237.

118.   Badyal, J. P.; Cameron A. M.; Cameron, N. R.; Coe, D. M.; Cox, R.; Davis B.G.; Oates, L. J.; Oye, G.; Steel, P. G. A simple method for the quantitative analysis of resin bound thiol groups. *Tetrahedron Lett*. **2001**, *42*, 8531-8533.